Electronic Supplementary Material (ESI) for Chemical Communications.

Supporting Information for:

Platination of Cysteine by an Epidermal Growth Factor Receptor Kinase-Targeted Hybrid Agent

Mu Yang, Hanzhi Wu, Julie Chu, Lucas A. Gabriel, Youngjoo Kim, Karen S. Anderson, Cristina M. Furdui and Ulrich Bierbach

Contents **Page**

1. Experimental Details

(a) General Supplies and Procedures

Methyl-3,4-dihydroxybenzoate (**1b**) (from 3,4-dihydroxybenzoic acid, **1a**) and *tert*-butyl(2-chloroethylmethyl)carbamate (**1l**) were synthesized according to published procedures.[1, 2] The platinum precursors **2a** and **2b**[3] and the quinazoline derivative **T1**[4] were synthesized as described previously. Potassium tetrachloroplatinate was from Acros. *N*-(3-Chloro-4-fluorophenyl)-7-methoxy-6-(3-morpholin-4-ylpropoxy)quinazolin-4-amine (gefitinib) was purchased from Sigma. The synthetic custom octapeptide (> 90% purity), QLMPFGCL, was purchased from Thermo Scientific/Pierce Protein Research (Rockford, IL). Incubations of the peptide with compounds **3** and **4** and sample work-ups were carried out as described for analogous gold(I) compounds previously.[4] For the preparation of biological buffers, biochemical grade reagents (Fisher/Acros) were used. HPLC-grade solvents were used for all HPLC and mass spectrometry experiments. All other reagents and chemicals were acquired from common vendors and used without further purification. ^{1}H NMR spectra of the target compounds and intermediates were recorded on Bruker Advance 300 and DRX-500 instruments. Proton-decoupled ^{13}C NMR spectra were recorded on a Bruker DRX-500 instrument operating 125.8 MHz. (Signal multiplicities in peak listings reflect ^{13}C–^{19}F coupling. [J(^{13}C–^{19}F) values are not reported.) Chemical shifts (δ) are reported in parts per million (ppm) relative to tetramethylsilane (TMS). Electrospray mass spectra (ES-MS) were recorded on an Agilent 1100LC/MSD trap instrument. Ion evaporation was assisted by a flow of N_2 drying gas (300−350 °C) at a pressure of 40−50 psi and a flow rate of 11 L/min. Mass spectra were typically recorded in positive-ion mode with a capillary voltage of +2800 V over a mass-to-charge (m/z) scan range of 200−2200. The purity and stability of the target compounds was analyzed by reverse-phase high-performance liquid

chromatography (HPLC) using the LC module of the Agilent Technologies 1100 LC/MSD trap system equipped with a multi-wavelength diode-array detector. Separations were accomplished with a 4.6 mm × 150 mm reverse-phase Agilent ZORBAX SB-C18 (5 μm particle size) analytical column at 25 °C and the following solvent system: solvent A–optima water/0.1% formic acid; solvent B–methanol/0.1% formic acid. Separations were performed at a flow rate of 0.5 mL/min and a gradient of 95% A/5% B to 5% A/95% B over 20 min (for all HPLC chromatograms). HPLC traces were recorded over a wavelength range of 363−463 nm.

(b) Synthetic Procedures for Intermediates and Target Compounds

Synthesis of $C_{22}H_{32}Cl_2FN_8OPt \cdot NO_3$ (1). A mixture of *cis*-[PtCl(EtCN)$(NH_3)_2$]NO_3 (**2a**) (0.1 g, 0.26 mmol) and N^4-(3-chloro-4-fluorophenyl)-7-ethoxy-N^6-(2-(methylamino)ethyl)-quinazoline-4,6-diamine (**T1**) (0.12 g, 0.31 mmol) in 1 mL of anhydrous DMF was stirred at 4 °C for 24 h. After the reaction warmed up to room temperature, di-tert-butyl dicarbonate (Boc_2O) (0.068 g, 0.31 mmol) was added and the reaction mixture was stirred for 1 h to deplete unreacted **T1**. The resulting solution was then added to 100 mL of vigorously stirred anhydrous diethyl ether. Compound **1** was recovered as a light-yellow microcrystalline precipitate, which was recrystallized repeatedly from hot ethanol until an analytical purity of greater than 95% was achieved. Yield: 56 mg (28%). Analytical purity > 95% (by LC-MS). ^{1}H NMR (500 MHz, DMF-d_7) δ 9.63 (s, 1H), 8.50 (s, 1H), 8.35 (dd, *J* = 6.9, 2.5 Hz, 1H), 7.94 (ddd, *J* = 9.0, 4.3, 2.6 Hz, 1H), 7.56 (s, 1H), 7.43 (t, *J* = 9.1 Hz, 1H), 7.17 (s, 1H), 6.07 (s, 1H), 5.92 (s, 1H), 4.55 (s, 3H), 4.32 (q, *J* = 7.1 Hz, 2H), 4.18 (s, 3H), 3.78 (d, *J* = 6.5 Hz, 2H), 3.63 (q, *J* = 6.6, 6.1 Hz, 2H), 3.31 – 3.06 (m, 5H), 1.48 (t, *J* = 6.9 Hz, 3H), 1.35 (t, *J* = 7.6 Hz, 3H). ^{13}C{^{1}H} NMR (126 MHz, DMF-d_7) δ 170.58, 156.24, 154.99, 153.06, 153.00, 151.14, 145.75, 139.59, 138.57, 123.72, 122.38, 119.88,

116.98, 111.30, 106.94, 97.39, 65.12, 50.52, 41.64, 28.16, 14.68, 11.84, 11.52. ESI-MS (positive-ion mode) for $[M]^+$: m/z 709.22; calcd. 709.17.

Synthesis of $C_{28}H_{42}Cl_2FN_8OPt \cdot NO_3$ (2). This derivative was generated by the same procedure as compound **1**. Starting from [PtCl(EtCN)(tmeda)]NO_3 (**2b**) (0.1 g, 0.215 mmol) and **T1** (0.1g 0.26 mmol), compound **2** was isolated as a yellow solid. Yield 0.057 g (31%). Analytical purity > 95% (by LC-MS). ^{1}H NMR (500 MHz, MeOH-d_4) δ 8.36 (s, 1H), 7.99 (dd, J = 6.7, 2.6 Hz, 1H), 7.69 – 7.64 (m, 1H), 7.33 – 7.20 (m, 2H), 7.06 (s, 1H), 5.51 (s, 1H), 4.28 (q, J = 7.0 Hz, 2H), 3.78 (s, 2H), 3.68 (d, J = 5.7 Hz, 2H), 3.23 – 2.75 (m, 16H), 2.63 (s, 5H), 1.55 (t, J = 6.9 Hz, 3H), 1.30 (t, J = 7.6 Hz, 3H). ^{13}C NMR (126 MHz, MeOH-d_4) δ 170.53, 156.01, 155.45, 153.51, 152.43, 150.32, 143.87, 139.00, 136.26, 124.40, 122.51, 120.00, 116.07, 110.19, 104.90, 95.30, 64.45, 64.10, 53.40, 51.00, 50.63, 40.43, 28.76, 13.60, 13.49, 9.90. ESI-MS (positive-ion mode) for $[M]^+$: m/z 791.36; calcd. 791.25.

Synthesis of methyl 4-ethoxy-3-hydroxybenzoate (1c). Compound **1b** was synthesized according to a published procedure in quantitative yield.[2] Potassium carbonate (8.1 g, 0.059 mol) was added to a solution of **1b** (10 g, 0.059 mol) in 40 mL of DMF. The mixture was stirred for 20 min at 0 °C, and iodoethane (4.7 mL, 0.059 mol) was added dropwise. After the addition was complete, the mixture was stirred for another 12 h at room temperature. The mixture was passed through a Celite pad and the DMF was removed under reduce pressure. The residue was redissolved in ethyl acetate and washed with 1 M HCl. The combined organic phases were dried over magnesium sulfate and concentrated using rotary evaporation until the solution turned cloudy, and the mixture was stored at 4 °C to complete crystallization of the product. The precipitate was washed with diethyl ether and dried in a vacuum to afford **1c** as a white solid. Yield: 4.2 g (36%). ^{1}H NMR (500 MHz, DMSO-d_6) δ 9.35 (s, 1H), 7.41 (dd, J = 8.4, 1.6 Hz, 1H), 7.38 (d, J = 1.5 Hz,

2H), 6.99 (d, *J* = 8.4 Hz, 1H), 4.09 (q, *J* = 7.0 Hz, 2H), 3.79 (s, 3H), 1.35 (t, *J* = 7.0 Hz, 3H). ^{13}C NMR (126 MHz, DMSO-d_6) δ 166.50, 151.61, 146.82, 122.20, 121.93, 116.25, 112.75, 64.26, 52.19, 15.04.

Synthesis of methyl-3-(benzyloxy)-4-ethoxybenzoate (1d). To a solution of **1c** (3.05 g, 15.6 mmol) in 10 mL of DMF were added potassium carbonate (3.23 g, 23.4 mmol) and benzyl bromide (2.93 g, 2 mL, 17.2 mmol). The mixture was heated at 100 °C for 2 h. After cooling to room temperature, DMF was removed under reduced pressure. Water was added, and the product was extracted three times with ethyl acetate. The combined organic phases were dried over magnesium sulfate. The solvent was removed to give **1d** in quantitative yield. ^{1}H NMR (500 MHz, DMSO-d_6) δ 7.59 (dd, *J* = 8.5, 2.1 Hz, 1H), 7.55 (d, *J* = 2.0 Hz, 1H), 7.46 (d, *J* = 7.2 Hz, 3H), 7.40 (t, *J* = 7.4 Hz, 3H), 7.33 (t, *J* = 7.4 Hz, 1H), 7.08 (d, *J* = 8.5 Hz, 1H), 5.15 (s, 2H), 4.12 (q, *J* = 6.9 Hz, 2H), 3.81 (s, 3H), 1.35 (t, *J* = 7.0 Hz, 3H). ^{13}C NMR (126 MHz, DMSO-d_6) δ 166.35, 153.16, 147.91, 137.39, 128.87, 128.29, 128.04, 124.04, 122.05, 114.58, 112.78, 70.50, 64.47, 52.32, 15.01.

Synthesis of methyl-5-(benzyloxy)-4-ethoxy-2-nitrobenzoate (1e). Compound **1d** (0.5 g, 2.55 mmol) was dissolved in a minimum amount of glacial acetic acid. To this solution were slowly added 0.32 mL of concentrated HNO_3 (70%). The mixture was stirred at 50 °C for 3 h and then poured into ice water. The resulting precipitate was filtered off, washed with water, and dried in a vacuum at 60 °C to give **1e** as a yellow solid. Yield 0.7 g (83%). ^{1}H NMR (500 MHz, DMSO-d_6) δ 7.65 (s, 1H), 7.49 – 7.33 (m, 6H), 5.28 (s, 2H), 4.20 (d, *J* = 7.0 Hz, 2H), 3.82 (s, 3H), 1.35 (t, *J* = 6.9 Hz, 3H). ^{13}C NMR (126 MHz, DMSO-d_6) δ 165.76, 151.67, 150.33, 141.56, 136.38, 129.01, 128.67, 128.34, 120.34, 113.18, 108.79, 71.02, 65.38, 53.49, 14.77.

Synthesis of methyl 2-amino-4-ethoxy-5-hydroxybenzoate (1f) and 7-ethoxyquinazoline-4,6-diol (1g). In an oxygen-free atmosphere, a suspension of compound **1e** (4.66 g, 14.1 mmol) in 90 mL of argon-purged methanol was reacted at room temperature with hydrogen gas in the presence of 10% palladium on carbon catalyst until light-yellow **1e** disappeared and a white precipitate formed (approximately 10–12 h, monitored by TLC). Palladium on carbon was filtered off through a Celite pad and washed exhaustively with 400 mL of methanol. Methanol was removed from the highly air-sensitive filtrate to afford the amine **1f** as a white solid, which was used immediately in the next step without further purification to avoid oxidation. To a solution of **1f** in 60 mL of 2-methoxyethanol was added formamidine acetate (2.94 g, 28.2 mmol), the mixture was refluxed overnight in an argon atmosphere. The solvent was removed under reduced pressure and water was added. Compound **1g** was collected as a light-brown solid, which was washed with water and dried in a vacuum at 60 °C. Yield: 2.0 g, 69% yield. **1f**: ^{1}H NMR (300 MHz, DMSO-d_6) δ 8.22 (s, 1H), 7.09 (s, 1H), 6.29 (s, 1H), 6.19 (s, 2H), 3.98 (q, J = 6.9 Hz, 2H), 3.71 (s, 3H), 1.34 (t, J = 6.9 Hz, 3H). ^{13}C NMR (75 MHz, DMSO) δ 167.38, 153.22, 146.85, 136.56, 114.96, 100.23, 99.66, 63.28, 50.88, 14.49. **1g**: ^{1}H NMR (500 MHz, DMSO-d_6) δ 11.92 (s, 1H), 9.73 (s, 1H), 7.90 (s, 1H), 7.40 (s, 1H), 7.07 (s, 1H), 4.16 (q, J = 6.9 Hz, 2H), 1.39 (t, J = 6.9 Hz, 3H). ^{13}C NMR (126 MHz, DMSO-d_6) δ 160.47, 153.54, 147.05, 144.23, 143.36, 116.30, 109.20, 109.14, 64.45, 14.91.

Synthesis of 7-ethoxy-4-hydroxyquinazolin-6-yl acetate (1h). A solution of **1g** (2.0 g, 9.7 mmol) in 10 mL of acetic anhydride and 2 mL pyridine was heated at reflux for 4 h. The mixture was poured into ice water and the precipitate was collected, washed with water, and dried in a vacuum at 60 °C. Yield: 1.8 g (75%). ^{1}H NMR (300 MHz, DMSO-d_6) δ 12.18 (s, 1H), 8.07 (s, 1H), 7.74 (s, 1H), 7.25 (s, 1H), 4.19 (q, J = 6.9 Hz, 2H), 2.29 (s, 3H), 1.33 (t, J = 6.9 Hz, 3H).

^{13}C NMR (126 MHz, DMSO-d_6) δ 169.04, 160.31, 155.77, 149.27, 146.20, 139.54, 119.40, 115.94, 110.15, 65.02, 20.77, 14.69.

Synthesis of 4-chloro-7-ethoxyquinazolin-6-yl acetate (1i) and 4-((3-chloro-4-fluorophenyl)amino)-7-ethoxyquinazolin-6-yl acetate (1j). The highly reactive 4-chloroquinazoline intermediate **1i** was generated without further purification and characterization. A mixture of **1h** (2.3 g, 9.2 mmol), 13 mL of thionyl chloride, and 0.2 mL of dry DMF was heated at reflux for 2 h. Excess thionyl chloride was removed under reduced pressure, and the residue was dissolved in dichloromethane. The dark solution was added to a pad of alumina gel and the product was eluted with a mixture of dichloromethane and ethyl acetate (2:1). The resulting orange colored solution of **1i** was immediately concentrated to a few mL and combined with a solution of 3-chloro-4-fluoroaniline (1.33 g, 9.2 mmol) in 40 mL of isopropanol. The mixture was stirred at room temperature for 2 h. During this period a bright yellow precipitate formed, which was filtered off, washed with isopropanol, and dried in a vacuum to give **1j**·HCl. Yield: 2.23 g (64%). ^{1}H NMR (500 MHz, DMSO-d_6) δ 11.59 (s, 1H), 8.94 (s, 1H), 8.81 (s, 1H), 8.06 (dd, J = 6.8, 2.6 Hz, 1H), 7.75 (ddd, J = 8.9, 4.3, 2.6 Hz, 1H), 7.59 – 7.49 (m, 3H), 4.27 (q, J = 6.9 Hz, 2H), 2.38 (s, 3H), 1.41 (t, J = 6.9 Hz, 3H). ^{13}C NMR (126 MHz, DMSO-d_6) δ 168.85, 159.28, 157.14, 156.53, 154.57, 151.44, 140.99, 140.14, 134.56, 134.54, 126.80, 125.54, 125.49, 119.71, 119.56, 118.87, 117.45, 117.28, 107.45, 102.30, 65.89, 20.56, 14.47.

Synthesis of 4-((3-chloro-4-fluorophenyl)amino)-7-ethoxyquinazolin-6-ol (1k). A suspension of **1j**·HCl (3.10 g, 8.25 mmol) in 90 mL of methanol were added 9 mL of concentrated ammonium hydroxide solution. When the mixture was refluxed for 1 h, the suspension turned into a white slurry. The precipitate was collected by filtration, washed, and dried in a vacuum at 60 °C. Yield: 2.97 g (92%). ^{1}H NMR (500 MHz, DMSO-d_6) δ 9.60 (s, 1H), 8.47 (s, 1H), 8.22 (dd, J =

6.9, 2.6 Hz, 1H), 7.90 – 7.77 (m, 2H), 7.40 (t, *J* = 9.1 Hz, 1H), 7.19 (s, 1H), 4.23 (q, *J* = 6.9 Hz, 2H), 1.44 (t, *J* = 6.9 Hz, 3H). ^{13}C NMR (126 MHz, DMSO-d_6) δ 156.38, 154.32, 153.70, 152.39, 152.18, 152.17, 147.32, 146.29, 137.62, 137.60, 123.35, 122.32, 122.26, 119.16, 119.01, 116.96, 116.79, 109.83, 107.84, 105.91, 64.61, 14.81.

Synthesis of tert-butyl(2-((4-((3-chloro-4-fluorophenyl)amino)-7-ethoxyquinazolin-6-yl)oxy)ethyl)(methyl)carbamate (1m) and *N*-(3-chloro-4-fluorophenyl)-7-ethoxy-6-(2-(methylamino)ethoxy)quinazolin-4-amine (1n, **T2).** A mixture of (**1k**) (1.5 g, 4.5 mmol), *tert*-butyl(2-chloroethylmethyl)carbamate (**1l**) (1.74 g, 9.0 mmol), potassium carbonate (0.62 g, 4.5 mmol), and potassium iodide (0.75, 4.5 mmol) in 5 mL of dry DMF was heated with stirring at 60 °C for 24 h. During this period, two additional equivalents of **1l** were added to the mixture after 8 h and 16 h. After cooling to room temperature, DMF was removed under reduced pressure. The residue was redissolved in 10 mL of dichloromethane, and insoluble salts were removed by filtration. The filtrate was then concentrated and purified via flash chromatography (alumina gel, dichloromethane) to yield **1m** as a yellow oil, which was used in the subsequent deprotection step without further purification. **1m** was then treated with 2 mL of trifluoroacetic acid dissolved in 2 mL of anhydrous dichloromethane. The solution was stirred at room temperature for 1 h and monitored by TLC. Upon completion, dichloromethane and trifluoroacetic acid were removed in a vacuum. The residue was then dissolved in dichloromethane and washed with 1 M sodium hydroxide solution. The organic layer was dried over magnesium sulfate and concentrated to yield **1n** (**T2**) as an off-white solid. Yield: 0.2 g (12%, two steps). ^{1}H NMR (500 MHz, DMSO-d_6) δ 9.58 (s, 1H), 8.49 (s, 1H), 8.14 (d, *J* = 6.7 Hz, 1H), 7.86 (s, 1H), 7.83 – 7.77 (m, 1H), 7.44 (t, *J* = 9.1 Hz, 1H), 7.18 (s, 1H), 4.21 (q, *J* = 7.9, 7.3 Hz, 4H), 2.97 (t, *J* = 4.7 Hz, 2H), 2.41 (s, 3H), 1.42 (t, *J* = 6.9 Hz, 3H). ^{13}C NMR (126 MHz, DMSO-d_6) δ 156.46, 154.53, 154.25, 153.09, 153.07,

152.60, 148.76, 147.48, 137.31, 137.28, 123.90, 122.79, 122.74, 119.26, 119.11, 117.02, 116.85, 109.12, 108.36, 103.54, 69.05, 64.52, 50.44, 36.61, 14.84.

Synthesis of $C_{22}H_{31}Cl_2FN_7O_2Pt\cdot NO_3$ (3). This derivative was generated using the procedure reported for compound **1**. Compound **3** was generated from the platinum-nitrile precursor **2a** (0.1 g, 0.26 mmol) and **1n** (0.12 g, 0.312 mmol). Yield: 0.058 g (29%). Analytical purity > 95% (by LC-MS). ^{1}H NMR (500 MHz, DMF-d_7) δ 9.76 (s, 1H), 8.60 (d, J = 1.9 Hz, 1H), 8.35 (dd, J = 6.9, 2.4 Hz, 1H), 8.05 (s, 3H), 7.99 (s, 1H), 7.97 – 7.93 (m, 1H), 7.45 (td, J = 9.1, 1.9 Hz, 1H), 7.27 (s, 1H), 6.14 (s, 1H), 4.55 (s, 3H), 4.37 (t, J = 4.1 Hz, 2H), 4.31 (q, J = 5.9, 5.4 Hz, 2H), 4.19 (s, 3H), 4.00 (s, 2H), 3.49 (s, 3H), 1.54 (t, J = 6.9 Hz, 3H), 1.45 (s, 3H). ^{13}C NMR (126 MHz, DMF-d_7) δ 156.53, 154.49, 154.33, 154.20, 152.94, 152.56, 148.48, 147.81, 137.61, 123.16, 121.83, 119.31, 116.55, 109.16, 108.07, 102.64, 64.51, 56.70, 18.27, 14.23. ESI-MS (positive-ion mode) for $[M]^+$: m/z 710.26; calcd. 710.15.

Synthesis of $C_{22}H_{31}Cl_2FN_7OPt\cdot NO_3$ (4). To a suspension of 1,3-diaminopropanedichloroplatinum(II) ([$PtCl_2$(pn)], 0.10 g, 0.29 mmol) in 1 mL of dry DMF was added $AgNO_3$ (0.047 g, 0.28 mmol), the suspension was stirred at room temperature in the dark for 16 h. Precipitated AgCl was removed by syringe filtration and the filtrate was added to a solution of compound **1n** (0.136 g, 0.35 mmol) in 1 mL of DMF. The mixture was then allowed to react at room temperature overnight. Boc_2O (0.076 g, 0.35 mmol) was added and reacted for 1 h to convert unreacted **1n** into its protected (ether-soluble) form, and the product was precipitated in vigorously stirred diethyl ether. The solid was collected and recrystallized from ethanol until an analytical purity of greater than 95% was achieved to afford compound **4** as an off-white microcrystalline solid. Yield: 0.050 g (25%). Analytical purity > 95% (by LC-MS). ^{1}H NMR (500 MHz, DMF-d_7) δ 9.91 (s, 1H), 8.57 (s, 1H), 8.42 (dd, J = 7.0, 2.7 Hz, 1H), 8.26 (s, 1H), 7.39 (t, J

= 9.0 Hz, 1H), 7.25 (s, 1H), 6.39 – 5.37 (m, 6H), 5.16 – 4.81 (m, 6H), 4.61 – 4.41 (m, 1H), 4.36 – 4.12 (m, 4H), 3.57 (q, *J* = 7.3 Hz, 3H), 1.50 (t, *J* = 6.9 Hz, 3H). ^{13}C NMR (126 MHz, DMF) δ 156.57, 154.47, 154.11, 153.00, 152.54, 147.96, 147.80, 137.62, 123.30, 122.05, 119.22, 116.40, 109.22, 108.22, 103.65, 66.86, 64.56, 56.70, 53.58, 18.29, 14.08. ESI-MS (positive-ion mode) for $[M]^+$: m/z 695.21; calcd. 695.14.

(c) Kinase Affinity and Selectivity Assays

KINOME*scan* competition binding assays[5] were performed by DiscoveRx Corp. (Fremont, CA). Stock solutions of compounds **1** and **2** were prepared in DMSO and stored at –80 °C until they were further diluted with assay buffer to the appropriate concentrations for testing. Prior to the assays it was confirmed that the test compounds did not react with DMSO during the short duration of the experiments (< 3 h, room temperature). Affinity studies were performed with recombinant kinase domains labeled with DNA tags. A known active site-binding surrogate ligand was immobilized on a solid support. DNA-tagged kinase, immobilized ligand, and test compound (or DMSO as negative control) were then incubated until equilibrium was achieved. Kinase captured on the beads was quantified by qPCR. Relative amounts of kinase remaining on the beads in the presence of test compound compared to negative control are reported as percent of control. Inhibitors with high binding affinities result in a low percentage of residual, solid-bound kinase molecules compared to a negative control, whereas weak inhibitors result in higher percentages of undissociated protein. The selectivity index (S_{35}) was calculated as the number of mapped unique kinases (excluding mutants) that bind compound **1** strongly (< 35% of control) divided by the total number of kinases screened. Details of the assay procedure have been reviewed[5] and can also be found at discoverx.com. The phylogenetic tree image was generated using TREE*spot* Software

Tool and reprinted with permission from KINOME*scan*, a division of DiscoveRx Corporation (Fremont, CA, 2010).

(d) Enzyme Inhibition Assay

Kinase inhibition was tested in a mutant epidermal growth factor receptor tyrosine kinase, $EGFR_{L858R/T790M}$, using the Kinase-Glo assay platform (Promega, Madison, WI). Reactions were performed on black 96-well plates (BD Biosciences, San Jose, CA). Stock solutions (1 mM) in DMF were serially diluted with a customized 1× kinase reaction buffer (40 mM Tris-HCl, pH 7.5; 20 mM $MgCl_2$; 2 mM $MnCl_2$; 0.05 mM $Na_2S_2O_4$) that did not contain bovine serum albumin (BSA) and dithiothreitol (DTT). Reactions were assembled with 44 ng of kinase protein in 10 μL of buffer, 10 μL of 100 μM ATP/0.2 μg/μL poly(Glu_4Tyr_1) substrate, and 5 μL of inhibitor in 1× reaction buffer. Mixtures were incubated for 60 min and subsequently terminated by adding 25 μL of ADP-Glo reagent (Promega). Termination reactions were performed for 40 min, and 50 μL of kinase detection reagent (Promega) was added. After 30 min of incubation, the plates were analyzed for luminescence on a Synergy H1 Hybrid Reader (BioTek, Winooski, VT). IC_{50} values were calculated from a sigmoidal curve fit of the luminescence data using GraphPad Prism 5 (version 5.00, La Jolla, CA) for an average of two assays.

(e) Protein Digestion, Nano-LC-MS/MS, and Database Searching

Stock solutions (10 mM) of compounds **3** and **4** were diluted with 50 mM NH_4HCO_3 buffer to a final concentration of 22 μM. 10 μg of EGFR protein in 10 μL of 50 mM NH_4HCO_3 buffer was added to the test compound solution to establish a protein:TKI molar ratio of 1:10. The mixtures were incubated at 37 °C for 16 h and passed through a Bio-Gel P6 gel column to remove excess test compound. Proteins samples were digested with sequencing grade modified trypsin (Promega, Madison, WI) using a 1:20 enzyme-to-substrate ratio overnight at 37 °C on a shaker.

The tryptic peptides were acidified with 1% formic acid and desalted using a Thermo Scientific/Pierce C18 spin columns (cat #, 89873) according to the manufacturer's protocol. The peptide samples were dried using a SpeedVac Savant SPD1010 (Thermo).

Dried peptides were dissolved in 0.1% formic acid/5% acetonitrile (ACN). Samples (1 ug) were injected and separated on a Dionex Ultimate 3000 nanoLC system equipped with an Acclaim PepMap100 Nano-Trap Column (C18, 5 µm, 100Å, 100 µm i.d. × 2 cm nanoViper) and an Acclaim PepMap RSLC nanocolumn (C18, 2 µm, 100 Å, 75 µm i.d. × 15 cm, nanoViper) (Thermo Scientific). A flow rate of 300 nL/min with the following gradient was used: solvent A: 95% water, 5% ACN, 0.1% formic acid; solvent B: 20% water, 80% ACN, 0.1% formic acid; 0–5 min: 0–5% B; 5– 50 min: 5–45% B; 50–50.1 min: 45–90% B; 50.1–53 min: 90% B; 53-53.1 min: 90-5% B; 53.1–60 min, 5% B]. A Q Exactive HF mass spectrometer (Thermo Scientific) was used for MS/MS analysis. The spray voltage was 1.9 kV, and the temperature of the heated capillary was 250 °C. The instrument was operated in a data-dependent acquisition mode selecting the 20 most intense precursors from each scan. These peptide ions were fragmented by higher-energy collisional dissociation (HCD). The full-scan resolution was 60,000, and the MS/MS scan resolution was 15,000. Data were acquired using the XCalibur software (version 2.1). Protein identification was performed using Proteome Discoverer 1.3, and the protein sequence was downloaded in FASTA format from UniProt (http://www.uniprot.org/). Data files were searched against the downloaded database by using the following parameters: Enzyme: trypsin; max. missed cleavage sites: 2; search mode: MS/MS ion search with decoy database search included; modification: based on probe used in experiment; precursor mass tolerance: 10 ppm, fragment mass tolerance: 0.02 Da; target false discovery rate (FDR): 0.01.

2. Synthetic Schemes

Scheme S1. Synthesis of Anilinoquinazoline Derivative **T2** (Compound **1n**)

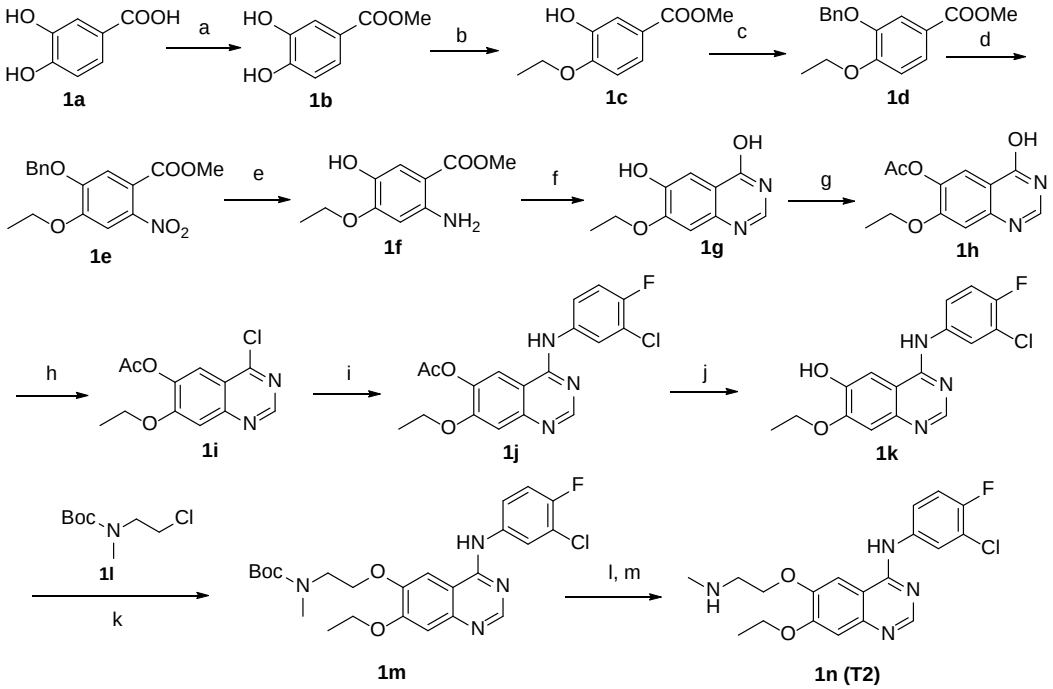

Reagents and conditions: (a) $SOCl_2$, MeOH, reflux, 1 h; (b) iodoethane, K_2CO_3, DMF, rt, overnight; (c) benzyl bromide, K_2CO_3, DMF, 100 °C, overnight; (d) conc. HNO_3, HOAc, 50 °C, 4 h; (e) Pd/C, H_2, MeOH, overnight; (f) formamidine acetate, ethanol, reflux, overnight; (g) acetic anhydride, pyridine, reflux, 2 h; (h) $SOCl_2$, reflux, 2 h; (i) 3-chloro-4-fluoroaniline, *i*-PrOH, rt, 3 h; (j) NH_4OH, MeOH, reflux, 1 h; (k) K_2CO_3, DMF, KI, 60 °C, overnight; (l) TFA, CH_2Cl_2; (m) aq. NaOH.

Scheme S2. Synthesis of Derivatives **1**–**4**.

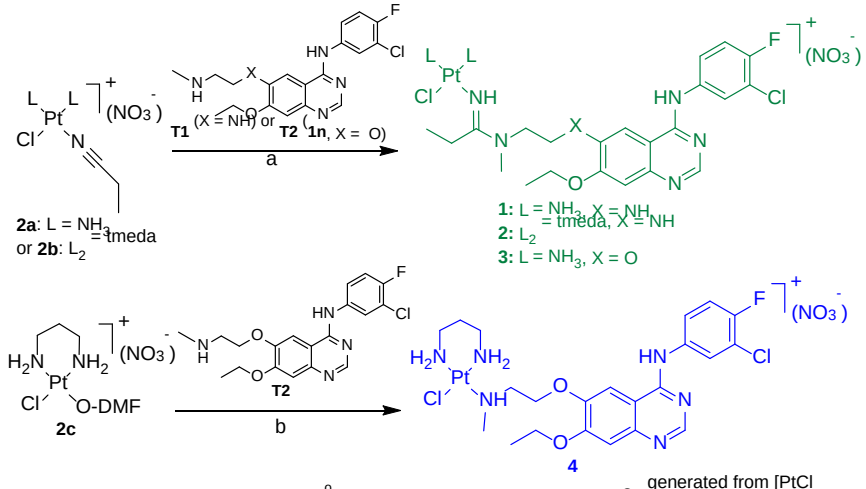

Reagents and conditions: (a) dry DMF, 4 °C, 24 h; (b) dry DMF, r.t., 24 h, from **2c** generated from $[PtCl_2(pn)]$ with 1 equiv. of $AgNO_3$, DMF, 16 h, rt)

3. LC-MS Analysis of Modified Octapeptide and MS/MS Analysis of Tryptic Digests of Modified EGFR Kinase

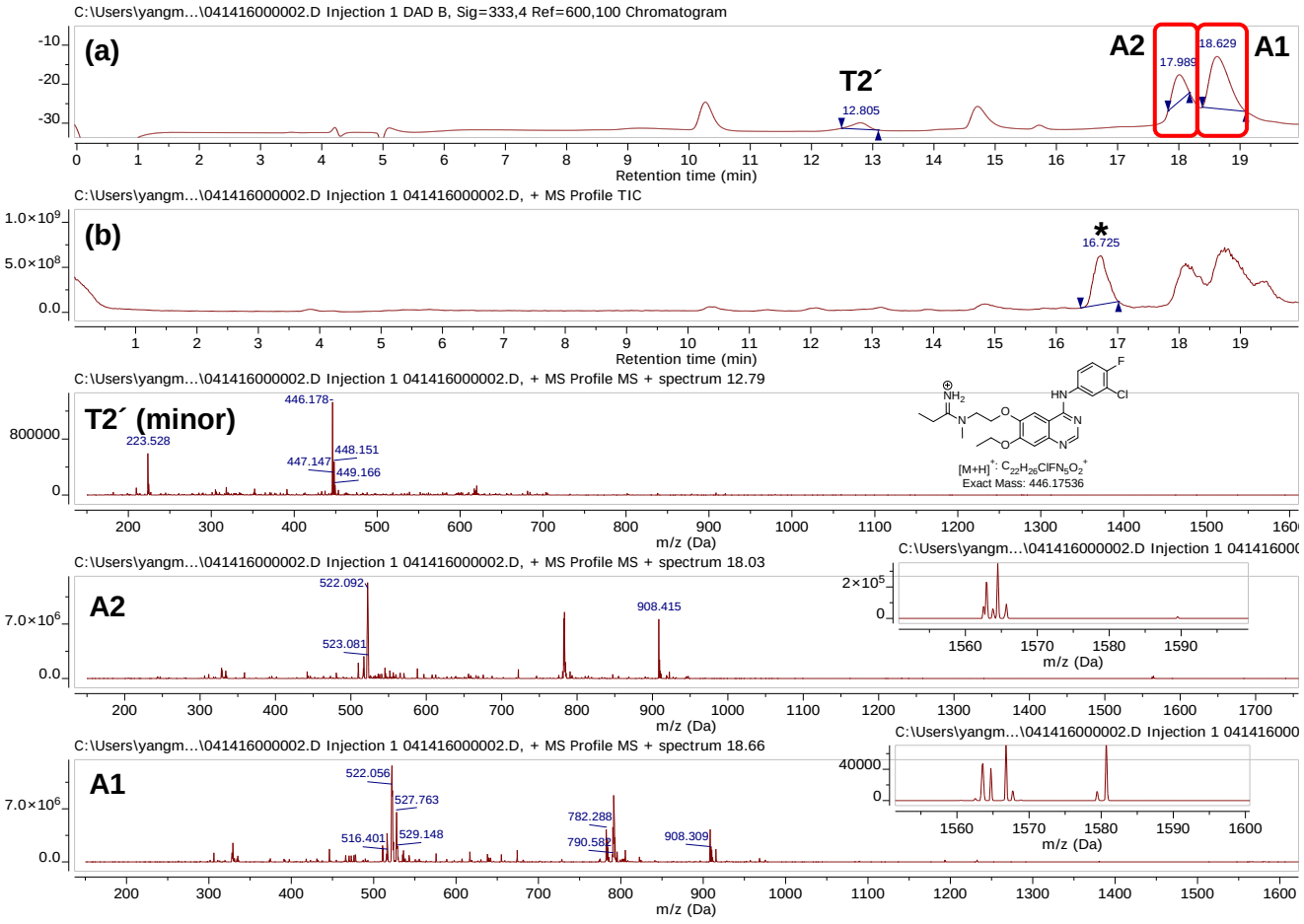

Figure S1. LC-MS results for the reaction of compound **3** with the octapeptide, QLMPFGCL. (a) and (b) are LC elution profiles monitored at 363–463 nm and as total ion current (TIC), respectively. The asterisk in the TIC trace indicates unmodified octapeptide. For details of adducts and in-source fragmentation see Table S1.

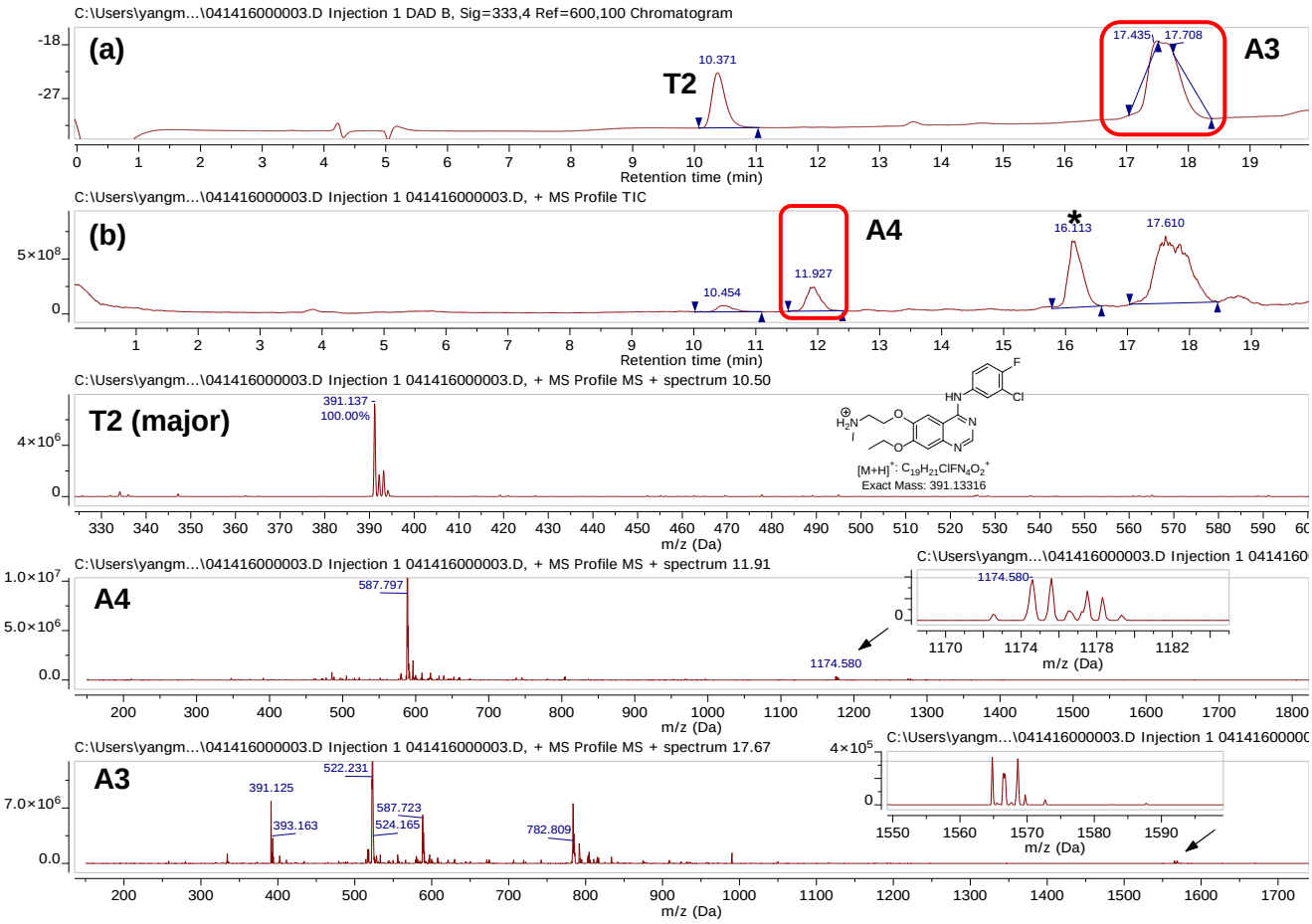

Figure S2. LC-MS results for the reaction of compound **4** with the octapeptide, QLMPFGCL. (a) and (b) are LC elution profiles monitored at 363–463 nm and as total ion current (TIC), respectively. The asterisk in the TIC trace indicates unmodified octapeptide. Note the overlapping LC peaks at retention times 17.4 and 17.7 min in (a) for the two diastereomeric forms of adduct **A3** (see text). For details of adducts and in-source fragmentation see Table S1.

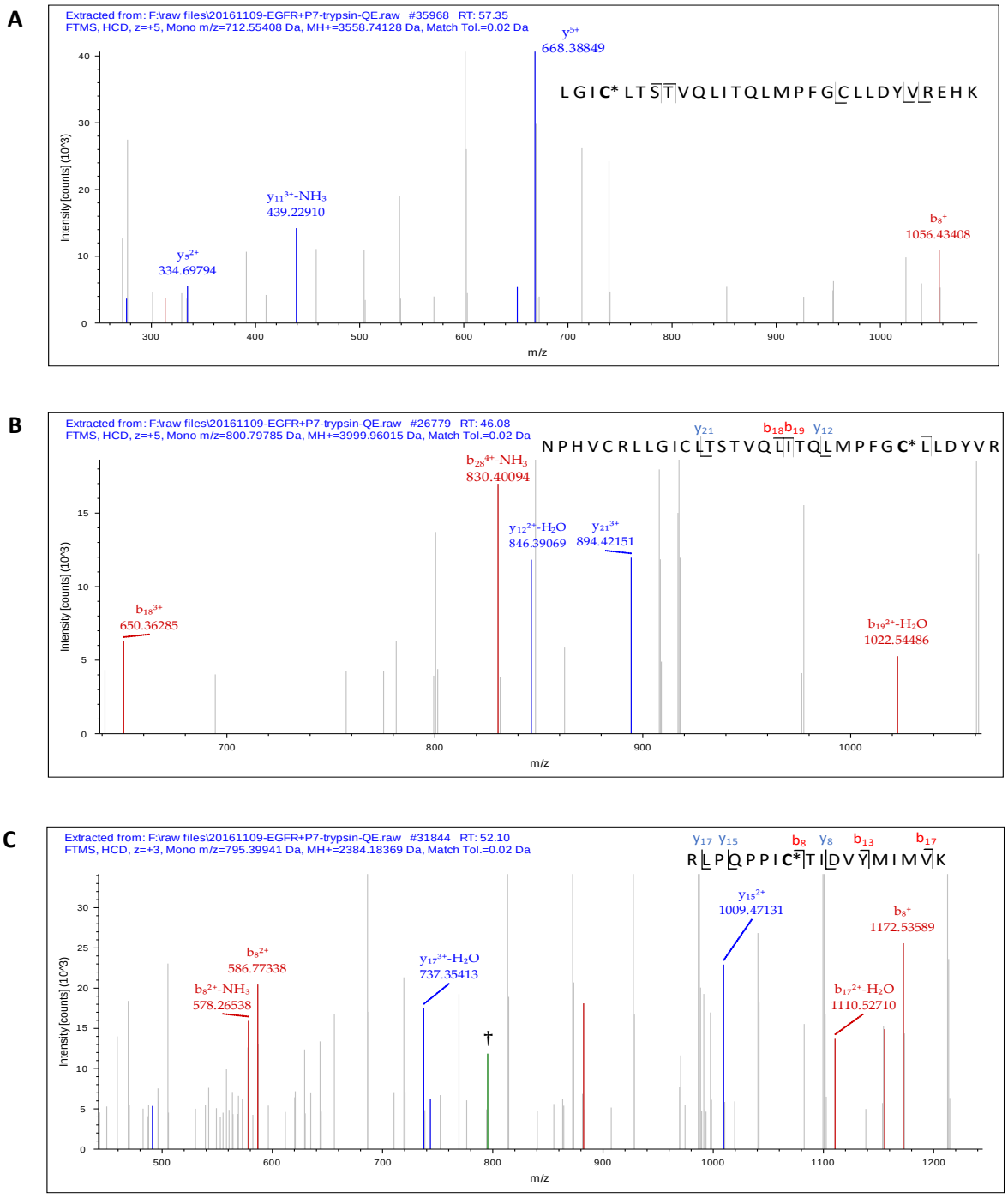

Figure S3. MS/MS for peptide fragments from tryptic digests of EGFR tyrosine kinase incubated with compound **4** with selected *b* and *y* fragments labeled: (A) L778 through K806, with C781 modified; (B) N771 through R803, with C797 modified; (C) R932 through K949, with C939 modified. The $[Pt(pn)]^{2+}$ fragment is indicated by an asterisk. The peak in (C) labeled with † is assigned to the precursor ion $[M+3H]^{3+}$. For a summary of peptides modified with the $[Pt(pn)]^{2+}$ fragment, precursor ions, and a complete list of *b* and *y* ions, see Table S2.

Table S1. Summary of LC-MS Results for Modified Octapeptide, QLMPFGC*L, and Fragments[a]

Modified Peptide	Assignment[b]	Calculated Mass (*m*/*z*)	Observed Mass (*m*/*z*)
A1	$[M]^{+}$	1580.61	1580.63
	$[M+H]^{2+}$	790.81	790.80
	$[M+2H]^{3+}$	527.74	527.76
A2	$[M+H]^{2+}$	782.29	782.29
	$[M+2H]^{3+}$	521.87	522.09
	$[QLMPFGCL+H]^{+}$	908.44	908.31
	$[M–NH_3]^{+}$	1563.58	1563.56
	$[M+2H–NH_3]^{3+}$	521.87	521.86
	$[M+2H–2NH_3]^{3+}$	516.19	516.18
	$[M+H–NH_3]^{2+}$	782.29	782.30
A3	$[M]^{+}$	1565.60	1565.56
	$[M+H]^{2+}$	783.30	783.32
	$[M+2H]^{3+}$	522.54	522.54
	$[M+H–\mathbf{T2}]^{2+}$	588.24	588.25
A4	$[M]^{+}$	1175.50	1175.59
	$[M+H]^{2+}$	588.24	588.25

Table S2. Summary of Tandem Mass Spectrometry Results for $[Pt(pn)]^{2+}$-Modified Peptides

Peptide Fragment[a]	Modified Residue	Precursor Ion $[MH]^+$ (m/z)	Observed b and y Ions[b]
		Model peptide	
QLMPFGC*L	C797	1175.47173	225.12364 (b_2^+–NH_3), 242.15028 (b_2^+), 356.16434 (b_3^+–NH_3), 373.19043 (b_3^+), **402.14771 (y_5^{2+})**, 453.21665 (b_4^+–NH_3), **467.66803 (y_6^{2+})**, **502.14460 (y_2^+)**, (514.18640 (b_7^{2+}–NH_3), 522.69147 (b_7^{2+}), **524.20955 (y_7^{2+})**, **559.16607 (y_3^+)**, 600.29053 (b_5^+–NH_3), 617.31162 (b_5^+), 657.30654 (b_6^+–NH_3), 674.33309 (b_6^+), **706.23590 (y_4^+)**, **803.28918 (y_5^+)**, **934.32990 (y_6^+)**, **1027.35181 (b_7^+–NH_3)**, **1044.37578 (b_7^+)**
		EGFR TK (tryptic digest)	
LGIC*LTSTVQLI-TQLMPFGCLLDY-VREHK	C781	3558.74128	276.16776 (y_4^{2+}–H_2O), **313.15021 (b_7^{3+}–H_2O)**, 334.69794 (y_5^{2+}), 439.22910 (y_{11}^{3+}–NH_3), 651.37646 (y_5^+–NH_3), 668.38849 (y_5^+), **1056.43408 (b_8^+)**
NPHVCRLLGICL-TSTVQLITQLMP-FGC*LLDYVR	C797	3999.96015	650.36285 (b_{18}^{3+}), **830.40094 (b_{28}^{4+}–NH_3)**, **846.39069 (y_{12}^{2+}–H_2O)**, **894.42151 (y_{21}^{3+})**, 1022.54486 (b_{19}^{2+})
RLPQPPIC*TIDV-YMIMVK	C939	2384.18369	491.23123 (y_8^{2+}), **578.26538 (b_8^{2+}–NH_3)**, **586.77338 (b_8^{2+})**, **737.35413 (y_{17}^{3+}–H_2O)**, **743.35681 (y_{17}^{3+})**, **882.42407 (b_{13}^{2+})**, **1009.47131 (y_{15}^{2+})**, **1110.52710 (b_{17}^{2+}–H_2O)**, **1155.50623 (b_8^+–NH_3)**, **1172.53589 (b_8^+–NH_3)**

[a] Modified cysteine residues in peptides are highlighted with an asterisk. [b] Fragments modified with the $[Pt(pn)]^{2+}$ chelate are highlighted in bold.

4. Kinase Binding and Inhibition Assays

Table S3. Complete List of Kinases and Primary Screening Results[a] of KINOME*Scan* Assay for Compound **1**

DiscoveRx Gene Symbol	Entrez Gene Symbol	Percent Control
ABL1(E255K)-phosphorylated	ABL1	73
ABL1(F317I)-nonphosphorylated	ABL1	81
ABL1(F317I)-phosphorylated	ABL1	64
ABL1(F317L)-nonphosphorylated	ABL1	94
ABL1(F317L)-phosphorylated	ABL1	65
ABL1(H396P)-nonphosphorylated	ABL1	52
ABL1(H396P)-phosphorylated	ABL1	75
ABL1(M351T)-phosphorylated	ABL1	67
ABL1(Q252H)-nonphosphorylated	ABL1	67
ABL1(Q252H)-phosphorylated	ABL1	64
ABL1(T315I)-nonphosphorylated	ABL1	98
ABL1(T315I)-phosphorylated	ABL1	71
ABL1(Y253F)-phosphorylated	ABL1	92
ABL1-nonphosphorylated	ABL1	85
ABL1-phosphorylated	ABL1	77
ABL2	ABL2	87
ALK	ALK	84
ALK(C1156Y)	ALK	86
ALK(L1196M)	ALK	89
AXL	AXL	84
BLK	BLK	44
BMX	BMX	92
BRK	PTK6	100
BTK	BTK	58
CSF1R	CSF1R	100
CSF1R-autoinhibited	CSF1R	79
CSK	CSK	88
CTK	MATK	100
DDR1	DDR1	97
DDR2	DDR2	100
EGFR	EGFR	0
EGFR(E746-A750del)	EGFR	0
EGFR(G719C)	EGFR	0
EGFR(G719S)	EGFR	0
EGFR(L747-E749del, A750P)	EGFR	0
EGFR(L747-S752del, P753S)	EGFR	5.8
EGFR(L747-T751del,Sins)	EGFR	0.6

EGFR(L858R)	EGFR	0.2
EGFR(L858R,T790M)	EGFR	14
EGFR(L861Q)	EGFR	0.05
EGFR(S752-I759del)	EGFR	1
EGFR(T790M)	EGFR	6.1
EPHA1	EPHA1	51
EPHA2	EPHA2	69
EPHA3	EPHA3	93
EPHA4	EPHA4	94
EPHA5	EPHA5	99
EPHA6	EPHA6	80
EPHA7	EPHA7	81
EPHA8	EPHA8	78
EPHB1	EPHB1	100
EPHB2	EPHB2	69
EPHB3	EPHB3	100
EPHB4	EPHB4	75
EPHB6	EPHB6	84
ERBB2	ERBB2	12
ERBB3	ERBB3	81
ERBB4	ERBB4	31
ERK2	MAPK1	99
FAK	PTK2	96
FER	FER	94
FES	FES	100
FGFR1	FGFR1	100
FGFR2	FGFR2	94
FGFR3	FGFR3	94
FGFR3(G697C)	FGFR3	92
FGFR4	FGFR4	100
FGR	FGR	84
FLT1	FLT1	77
FLT3	FLT3	32
FLT3(D835H)	FLT3	61
FLT3(D835Y)	FLT3	44
FLT3(ITD)	FLT3	41
FLT3(K663Q)	FLT3	61
FLT3(N841I)	FLT3	26
FLT3(R834Q)	FLT3	81
FLT3-autoinhibited	FLT3	100
FLT4	FLT4	82
FRK	FRK	79
FYN	FYN	97

GSK3B	GSK3B	81
HCK	HCK	40
IGF1R	IGF1R	89
IKK-beta	IKBKB	92
INSR	INSR	100
INSRR	INSRR	99
ITK	ITK	94
JAK1(JH1domain-catalytic)	JAK1	97
JAK1(JH2domain-pseudokinase)	JAK1	82
JAK2(JH1domain-catalytic)	JAK2	90
JAK3(JH1domain-catalytic)	JAK3	64
JNK1	MAPK8	82
JNK2	MAPK9	57
JNK3	MAPK10	78
KIT	KIT	95
KIT(A829P)	KIT	51
KIT(D816H)	KIT	65
KIT(D816V)	KIT	66
KIT(L576P)	KIT	100
KIT(V559D)	KIT	90
KIT(V559D, T670I)	KIT	99
KIT(V559D, V654A)	KIT	83
KIT-autoinhibited	KIT	84
LCK	LCK	26
LTK	LTK	90
LYN	LYN	53
MEK1	MAP2K1	89
MERTK	MERTK	89
MET	MET	75
MET(M1250T)	MET	100
MET(Y1235D)	MET	92
MST1R	MST1R	100
MUSK	MUSK	98
NEK2	NEK2	90
PDGFRA	PDGFRA	69
PDGFRB	PDGFRB	89
PYK2	PTK2B	84
RET	RET	77
RET(M918T)	RET	73
RET(V804L)	RET	87
RET(V804M)	RET	98
ROS1	ROS1	87
RSK1(Kin.Dom.1-N-terminal)	RPS6KA1	100

RSK2(Kin.Dom.1-N-terminal)	RPS6KA3	84
RSK3(Kin.Dom.1-N-terminal)	RPS6KA2	92
RSK4(Kin.Dom.1-N-terminal)	RPS6KA6	83
SRC	SRC	58
SRMS	SRMS	92
SYK	SYK	100
TAK1	MAP3K7	100
TEC	TEC	93
TIE1	TIE1	81
TIE2	TEK	92
TNK1	TNK1	100
TNK2	TNK2	73
TRKA	NTRK1	96
TRKB	NTRK2	98
TRKC	NTRK3	97
TXK	TXK	53
TYK2(JH1domain-catalytic)	TYK2	100
TYK2(JH2domain-pseudokinase)	TYK2	97
TYRO3	TYRO3	100
VEGFR2	KDR	90
YES	YES1	94
ZAP70	ZAP70	77

[a] Assay performed by DiscoveRx in 145 selected kinases; see Experimental Section for details. The 17 mapped targets are highlighted.

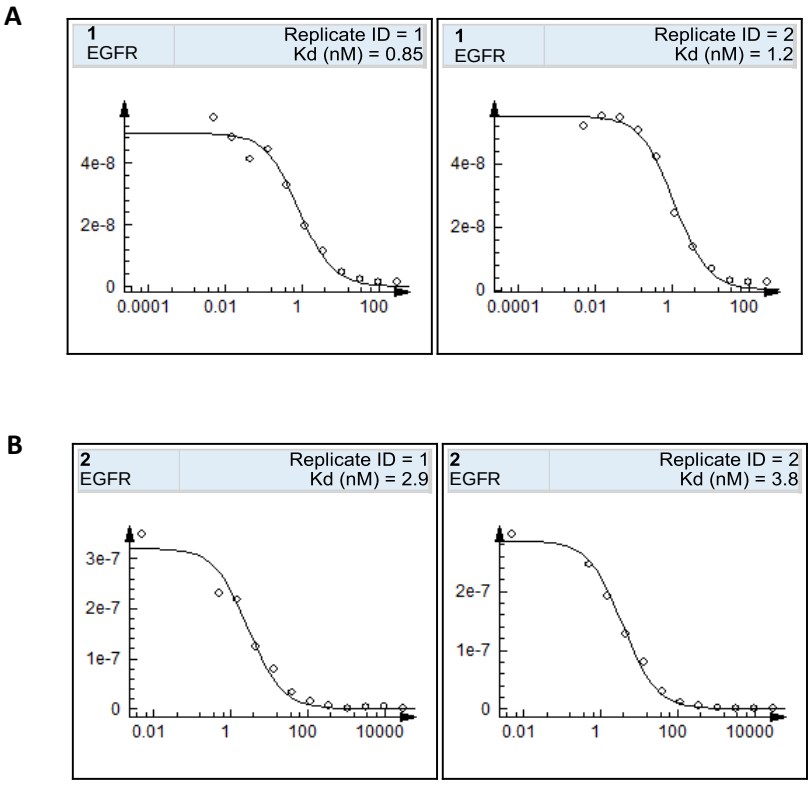

Figure S4. Binding affinity of compound **1** (A) and compound **2** (B) to wild-type EGFR kinase. Thermodynamic dissociation constants (K_d) for test compound–kinase interactions were determined in the absence of ATP and calculated by measuring the amount of kinase captured by an immobilized surrogate ligand as a function of the test compound concentration. Each measurement was performed in duplicate. The X axis represents logarithmic concentration of test compounds and the Y axis represents the intensity of qPCR signal, which is proportional to the amount of barcoded kinase captured by immobilized surrogate ligand (data acquired by DiscoveRx).

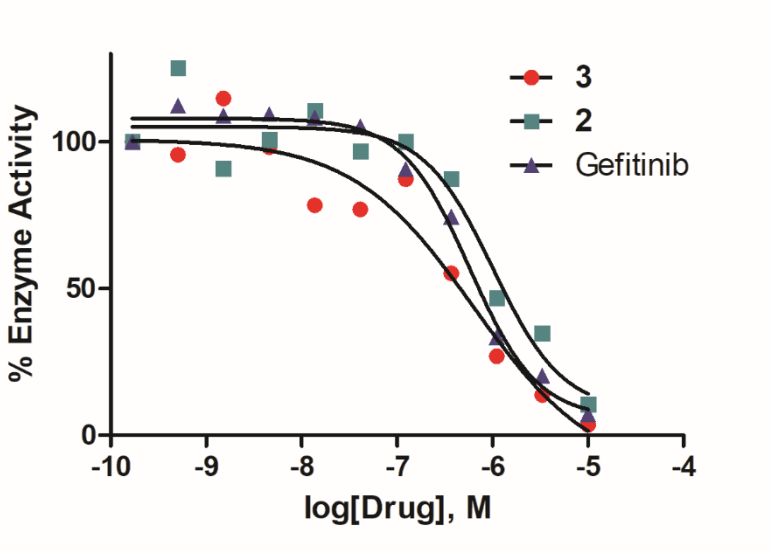

Figure S5. Inhibition of substrate phosphorylation by recombinant EGFR tyrosine kinase (L858R/T790M double mutant) in the presence of inhibitors **2**, **3**, and gefitinib monitored by an assay measuring conversion of ATP to ADP. Plotted data are averages of two determinations. IC_{50} values (from sigmoidal curve fits): gefitinib, 0.65 μM; **2**, 1.22 μM; **3**, 0.49 μM.

5. Supplementary Spectroscopic and Analytical Data

(a) ^{1}H and ^{13}C NMR spectra of intermediates and target compounds

(b) LC/MS profiles and purity analysis

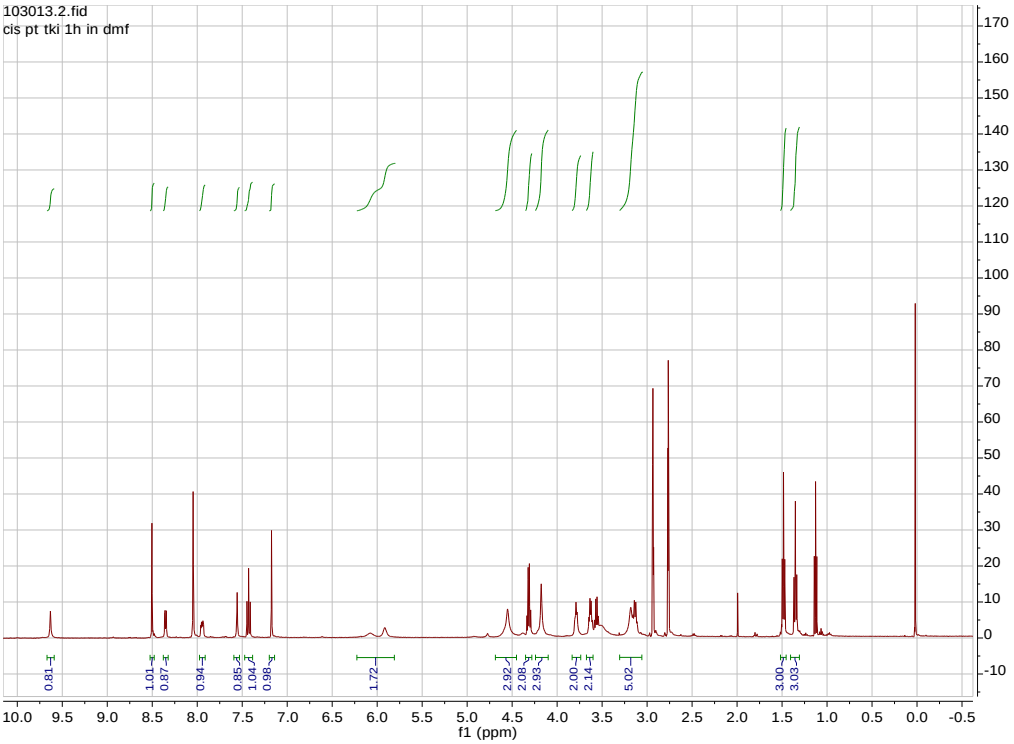

Figure S6. ^{1}H NMR spectrum of compound **1** in DMF-d$_7$.

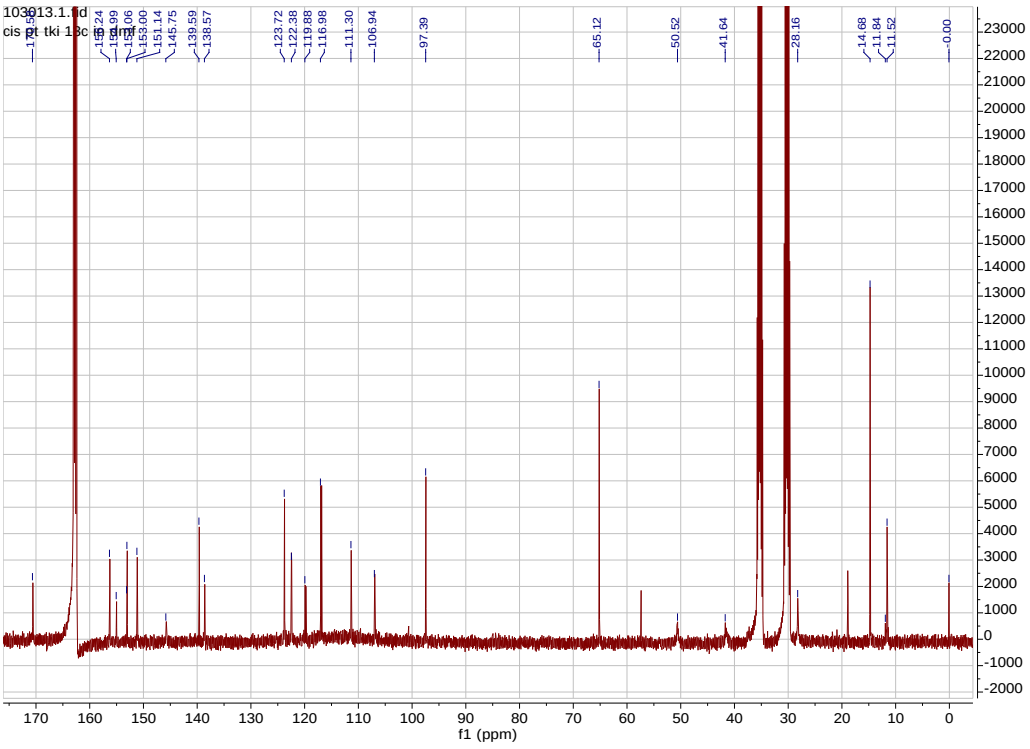

Figure S7. ^{13}C NMR spectrum compound **1** in DMF-d$_7$.

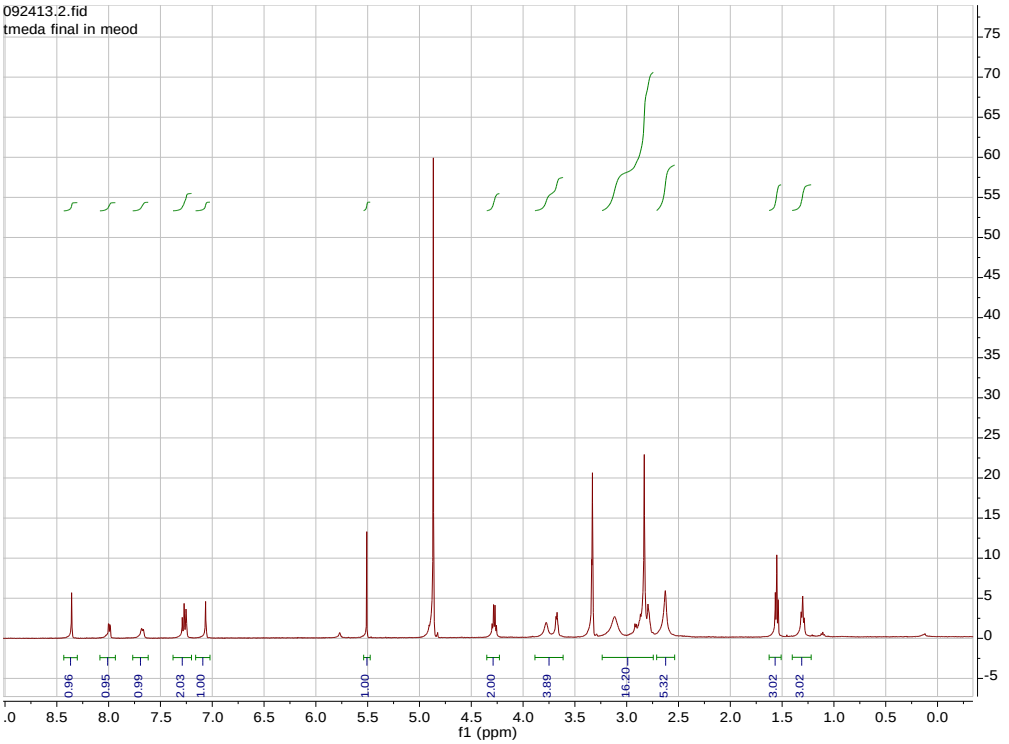

Figure S8. ^{1}H NMR spectrum of compound **2** in methanol-d_4.

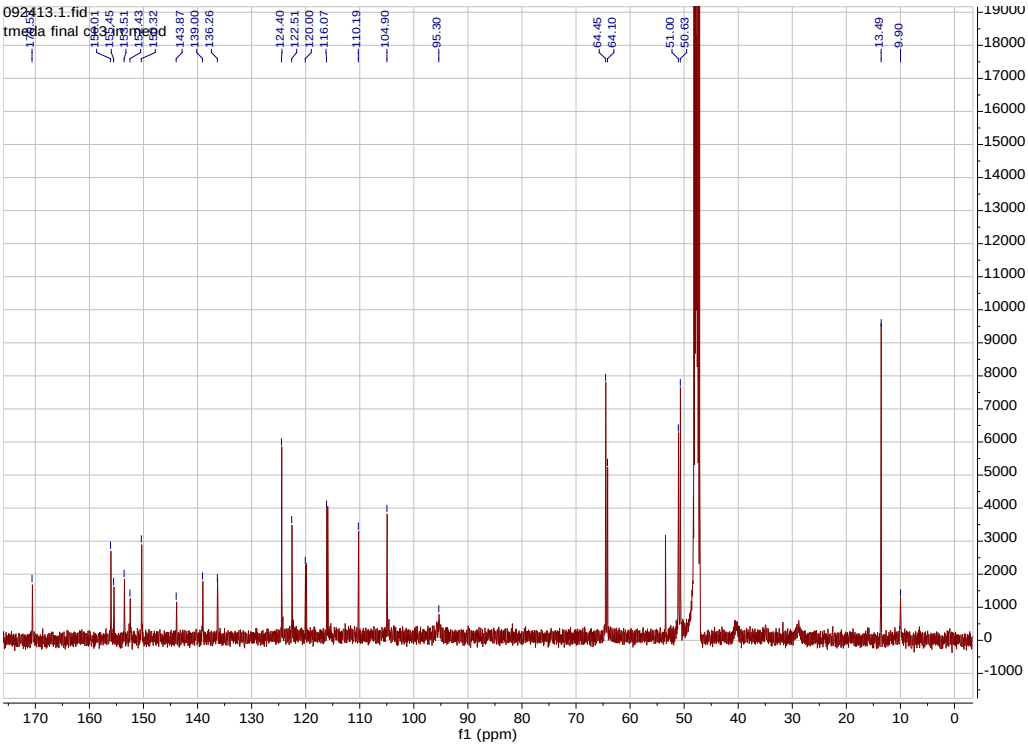

Figure S9. ^{13}C NMR spectrum of compound **2** in methanol-d_4.

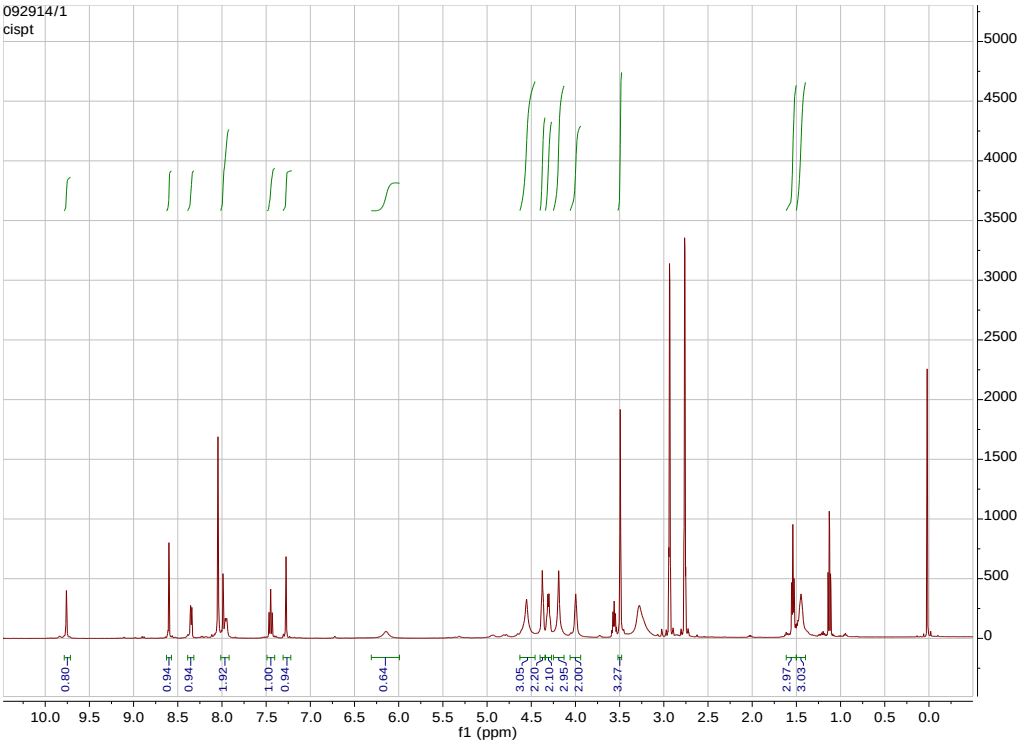

Figure S10. ^{1}H NMR spectrum of compound **3** in DMF-d_7.

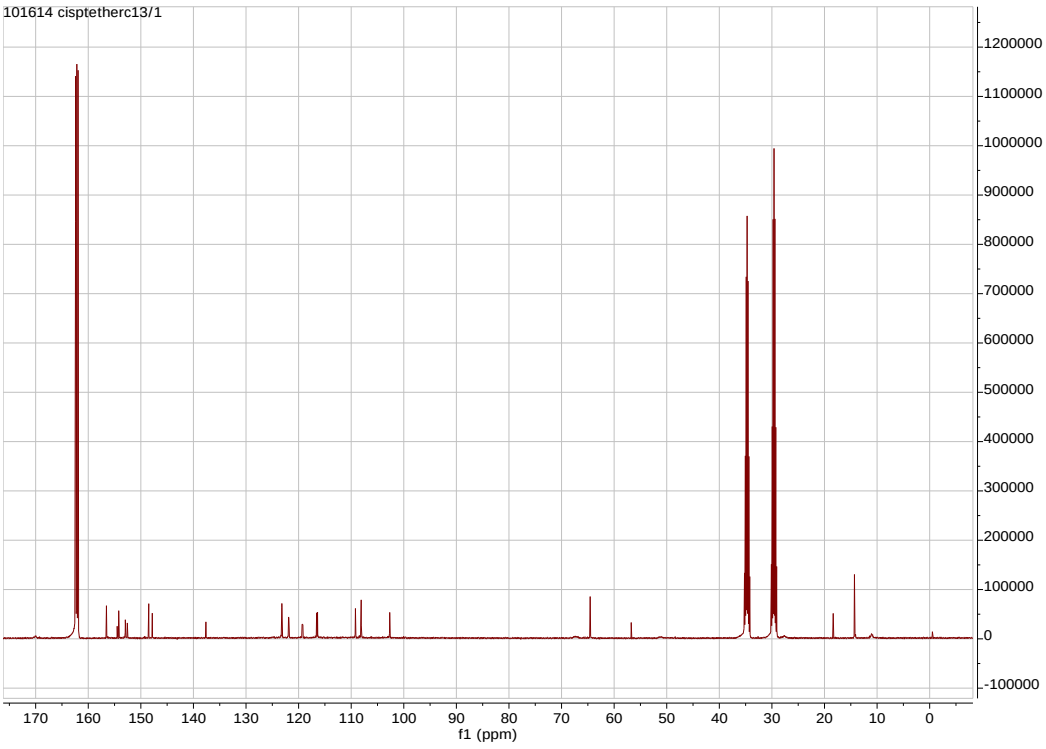

Figure S11. ^{13}C NMR spectrum of compound **3** in DMF-d_7.

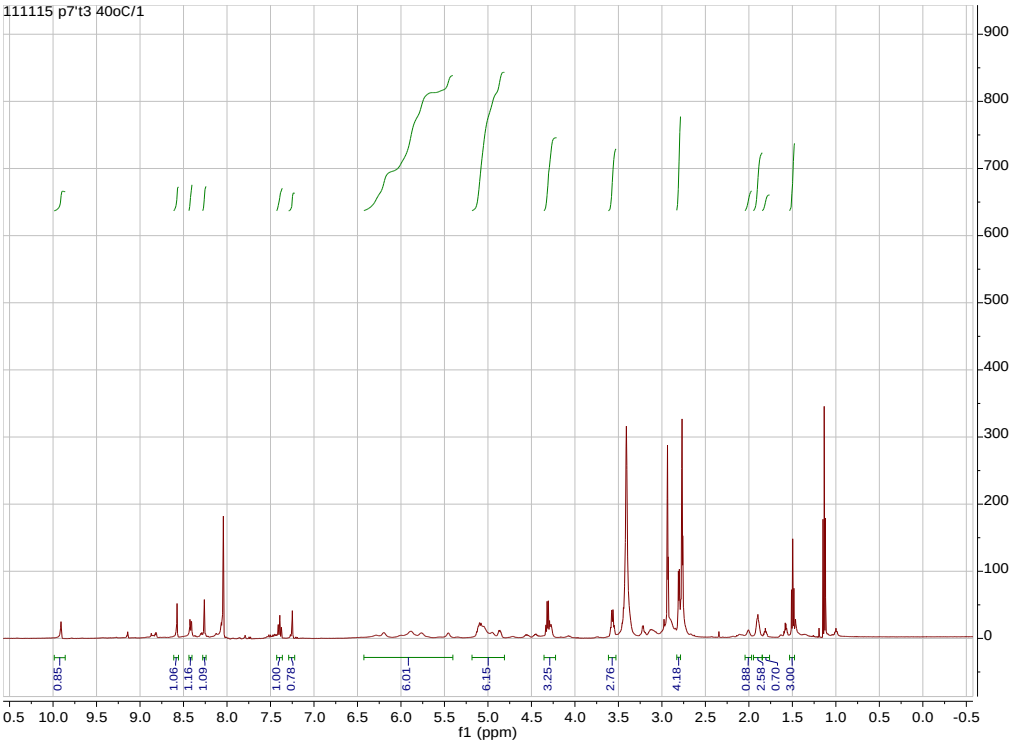

Figure S12. ^{1}H NMR spectrum of compound **4** in DMF-d_7.

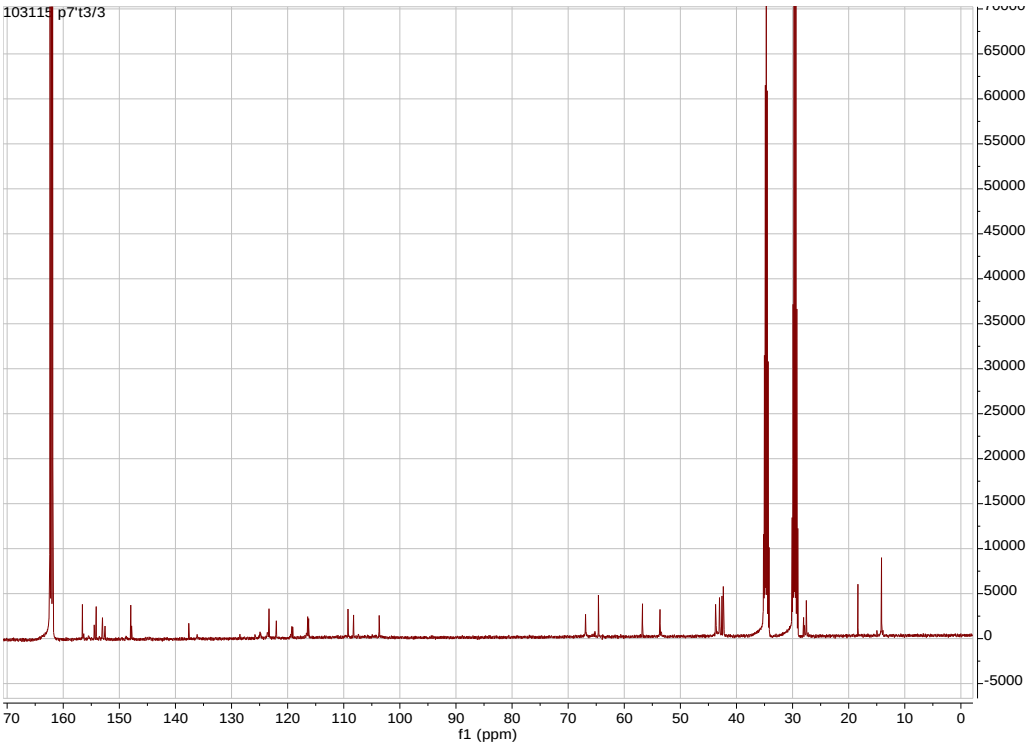

Figure S13. ^{13}C NMR spectrum of compound **4** in DMF-d_7.

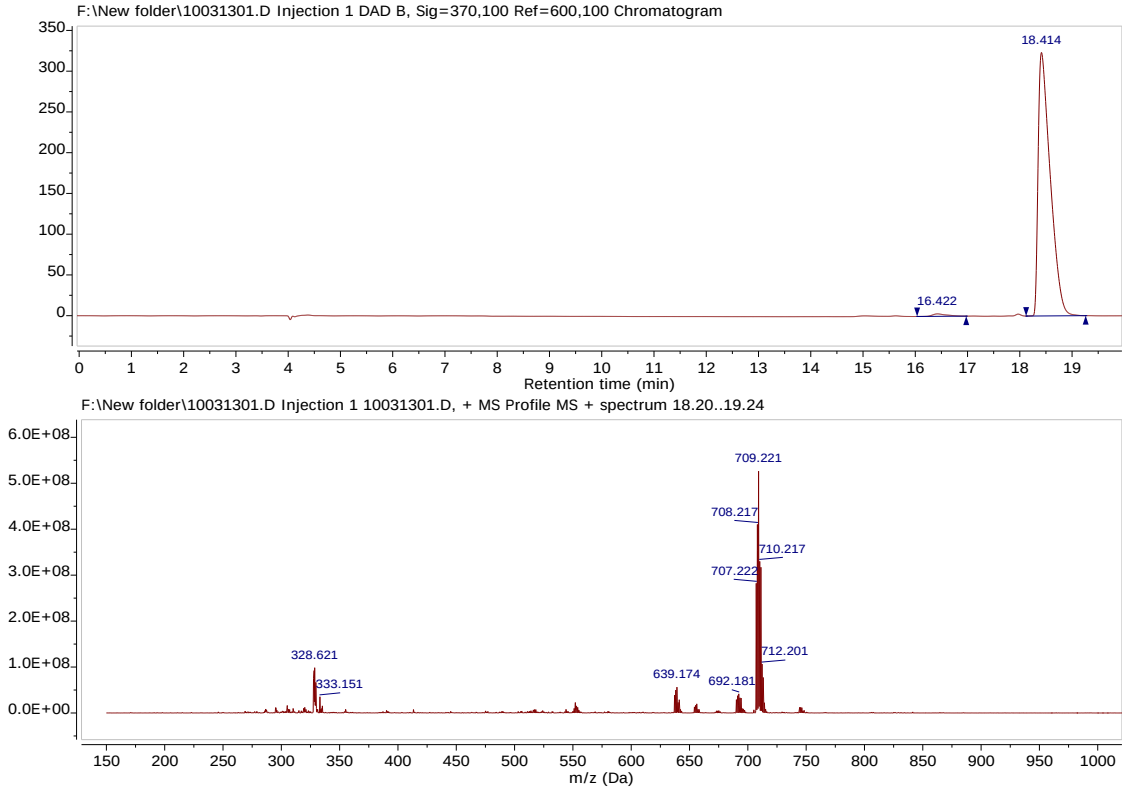

	RT	Total Area %	Start time	End time
1	18.414	98.92	18.121	19.261
2	16.422	1.08	16.035	16.975

Figure S14. LC-MS analysis and purity of compound **1**.

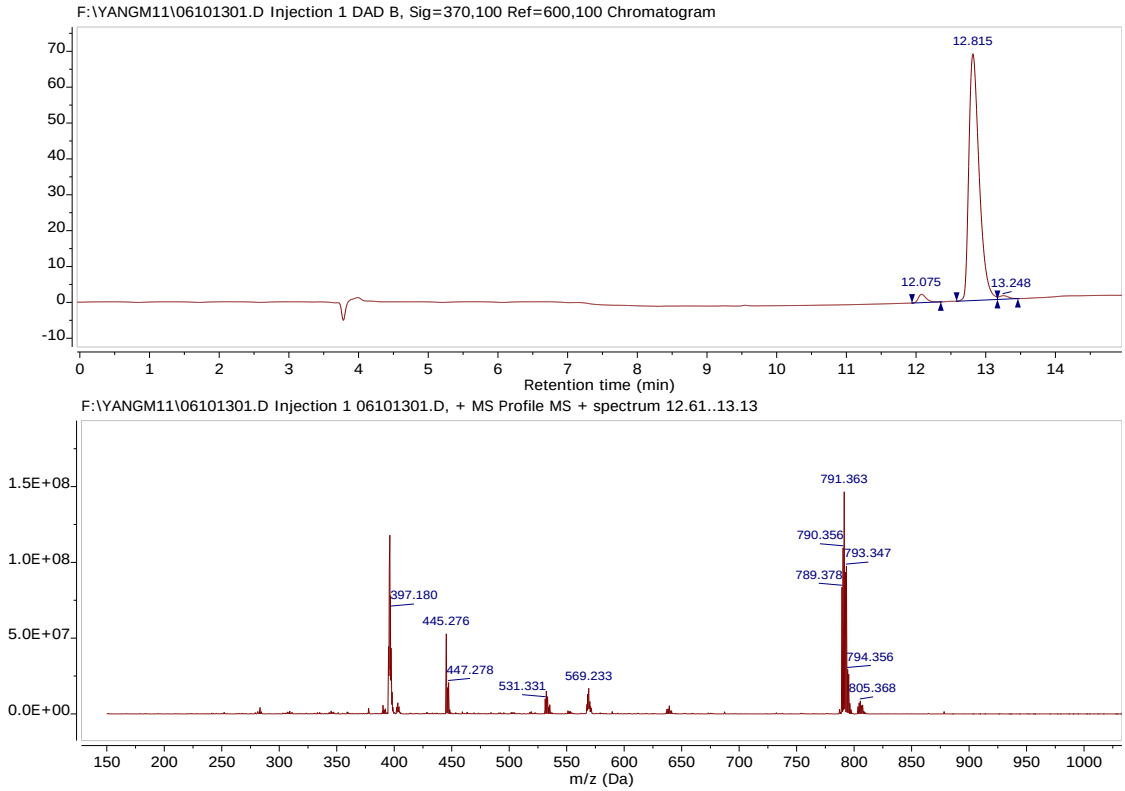

	RT	Total Area %	Start time	End time
1	13.248	1.26	13.168	13.461
2	12.815	96.25	12.582	13.168
3	12.075	2.49	11.942	12.355

Figure S15. LC-MS analysis and purity of compound **2**.

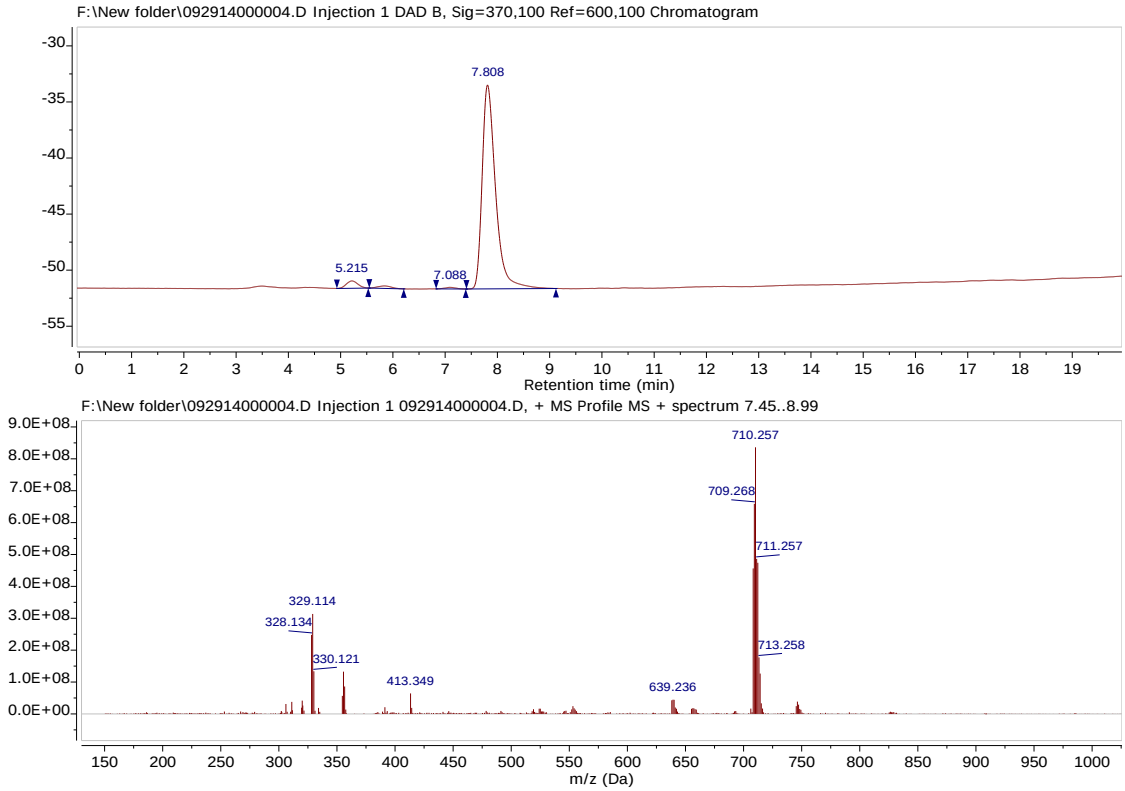

	RT	Total Area %	Start time	End time
1	7.808	95.23	7.408	9.121
2	7.088	0.61	6.828	7.395
3	5.842	1.19	5.548	6.208
4	5.215	2.97	4.929	5.528

Figure S16. LC-MS analysis and purity of compound **3**.

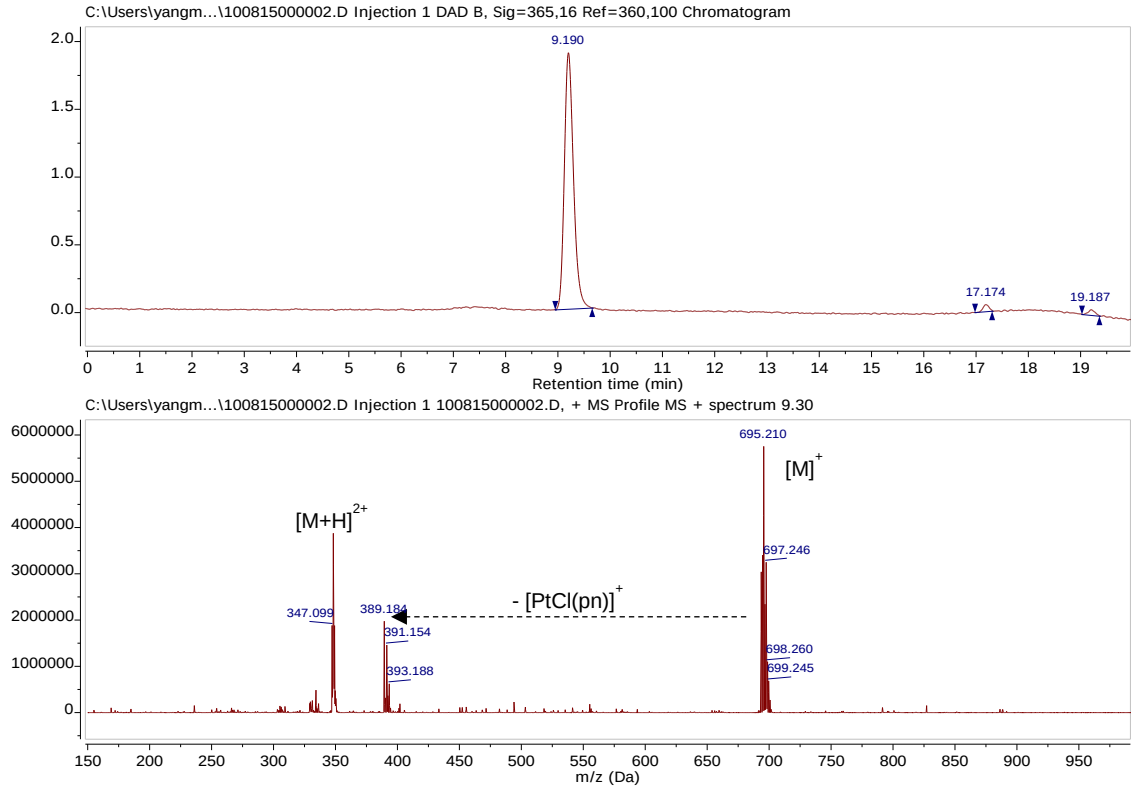

	RT	Total Area %	Start time	End time
1	19.187	1.61	19.027	19.360
2	17.174	1.84	16.981	17.307
3	9.190	96.54	8.950	9.657

Figure S17. LC-MS analysis and purity of compound **4**.

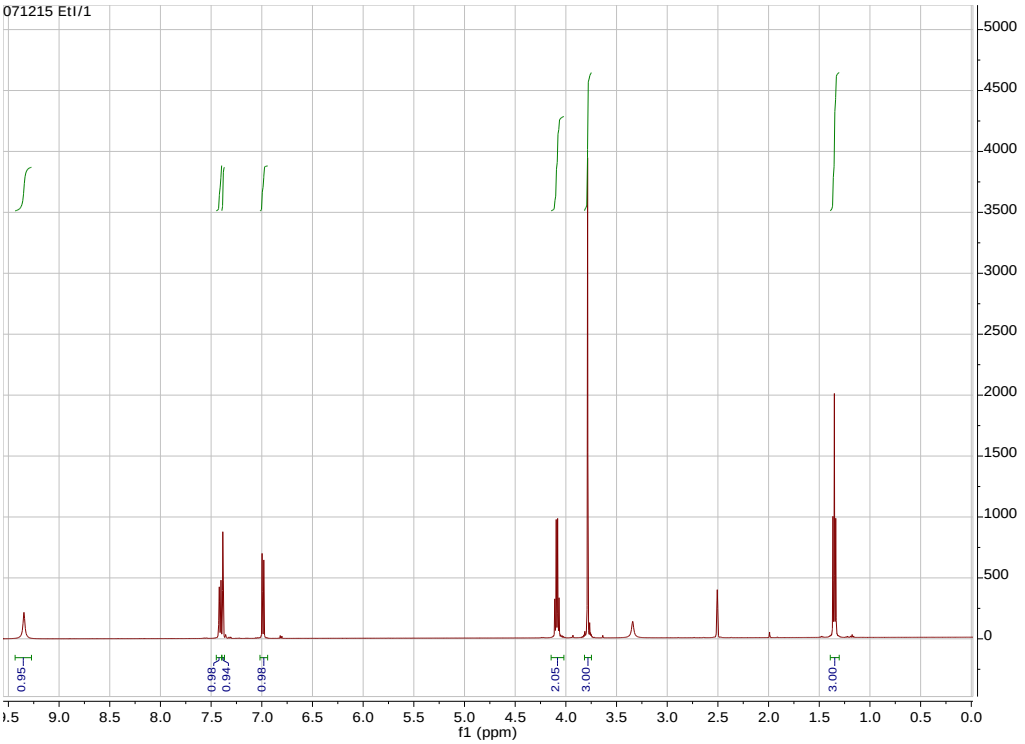

Figure S18. ^{1}H NMR spectrum of compound **1c** in DMSO-d_6.

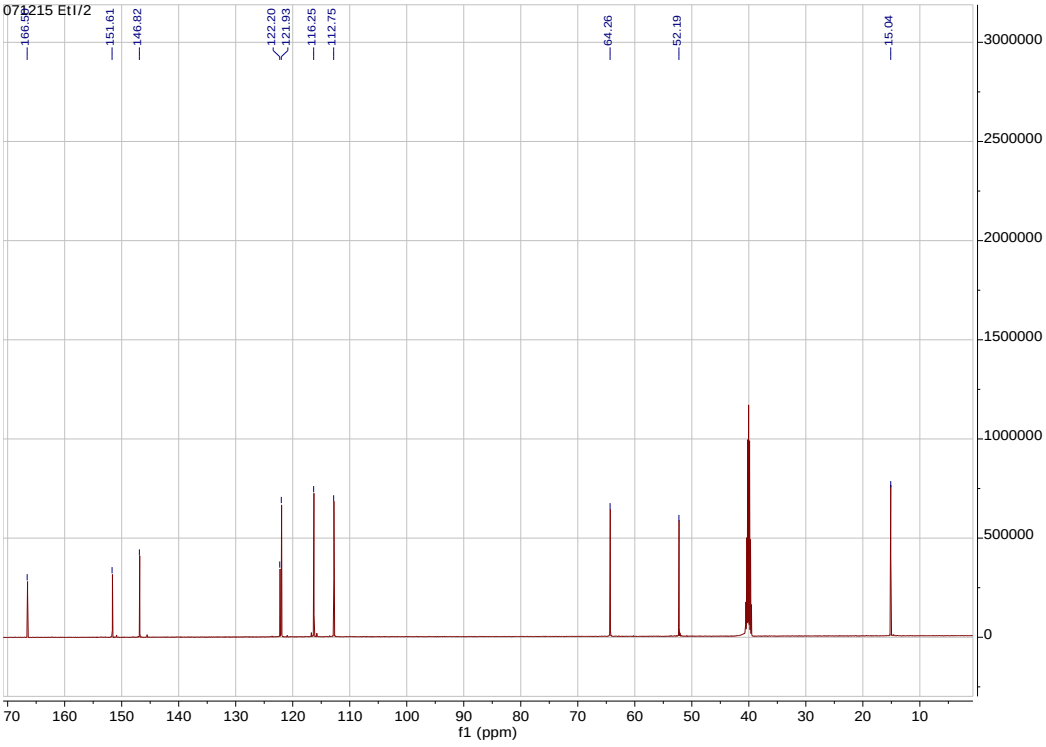

Figure S19. ^{13}C NMR spectrum of compound **1c** in DMSO-d_6.

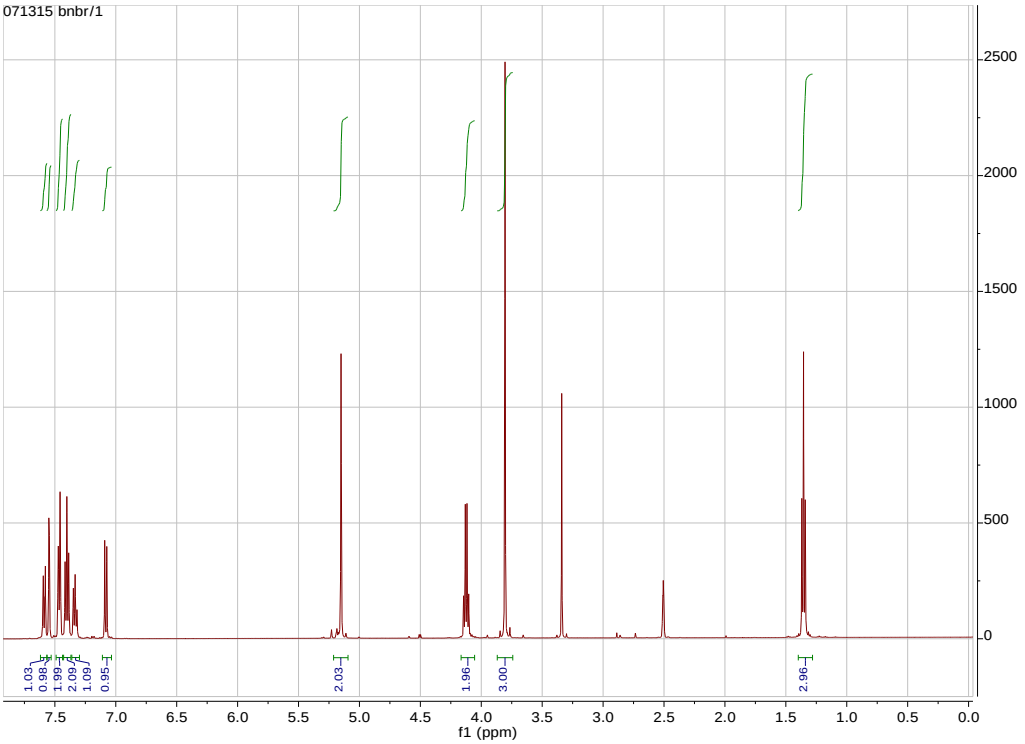

Figure S20. ^{1}H NMR spectrum of compound **1d** in DMSO-d_6.

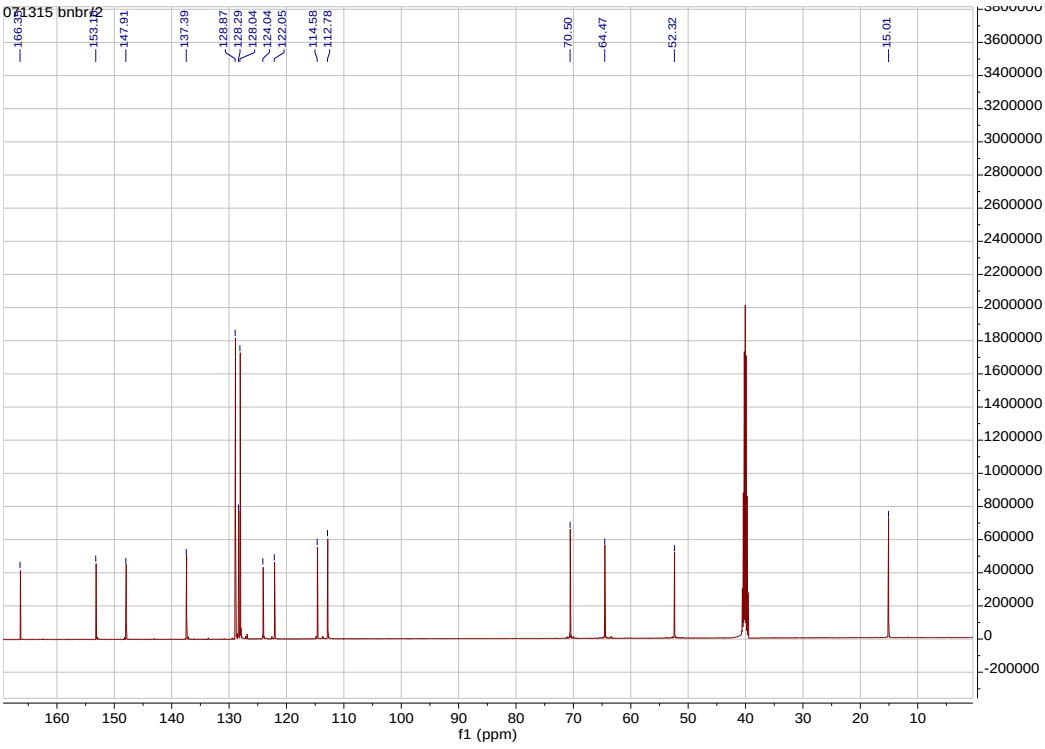

Figure S21. ^{13}C NMR spectrum of compound **1d** in DMSO-d_6.

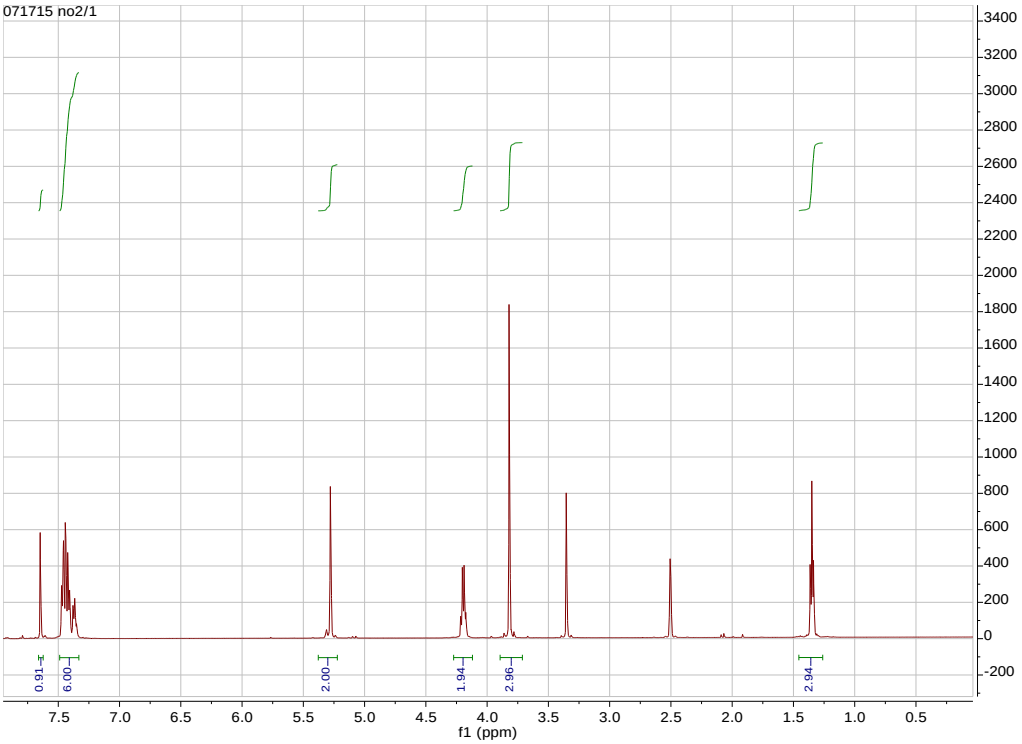

Figure S22. ^{1}H NMR spectrum of compound **1e** in DMSO-d_6.

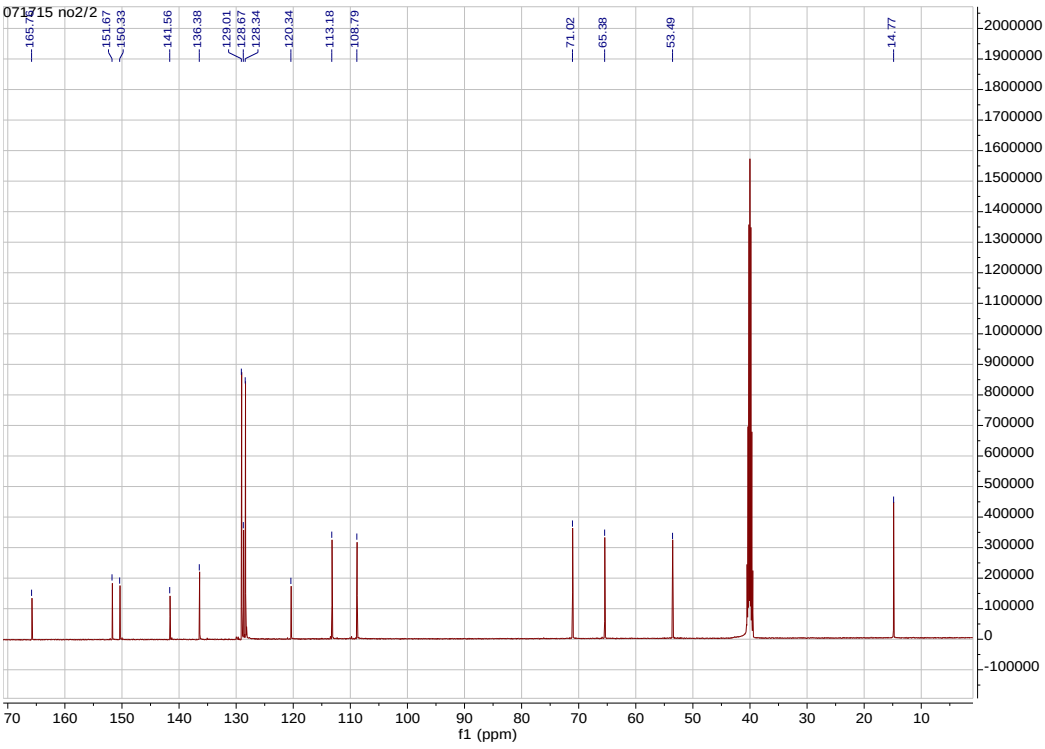

Figure S23. ^{13}C NMR spectrum of compound **1e** in DMSO-d_6.

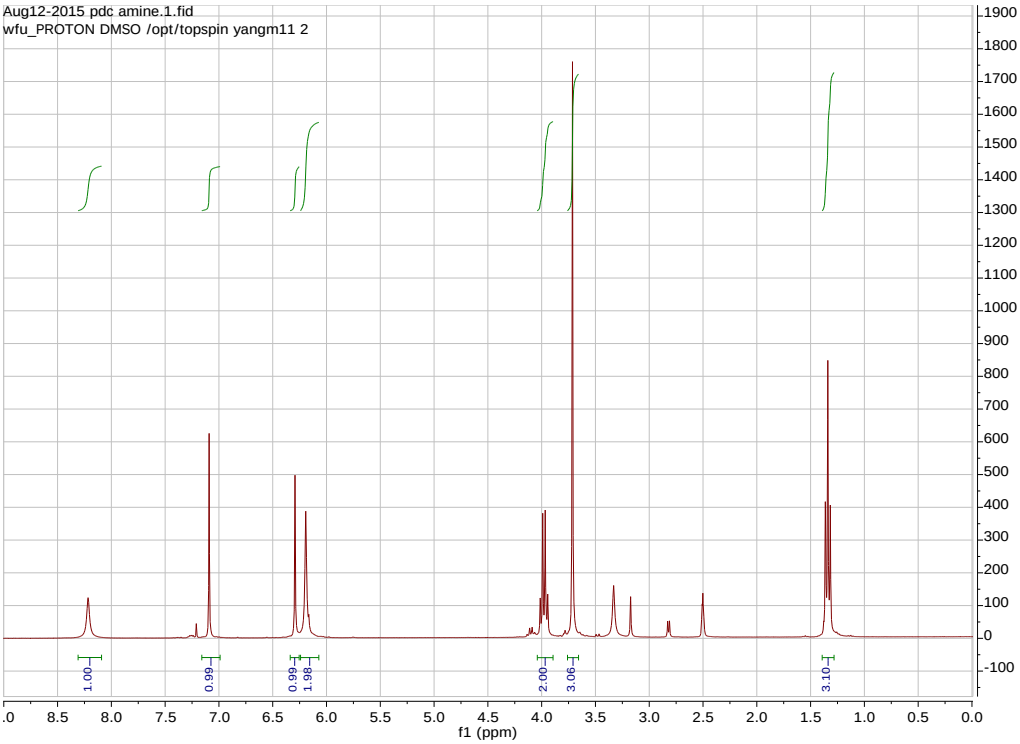

Figure S24. ^{1}H NMR spectrum of compound **1f** in DMSO-d_6.

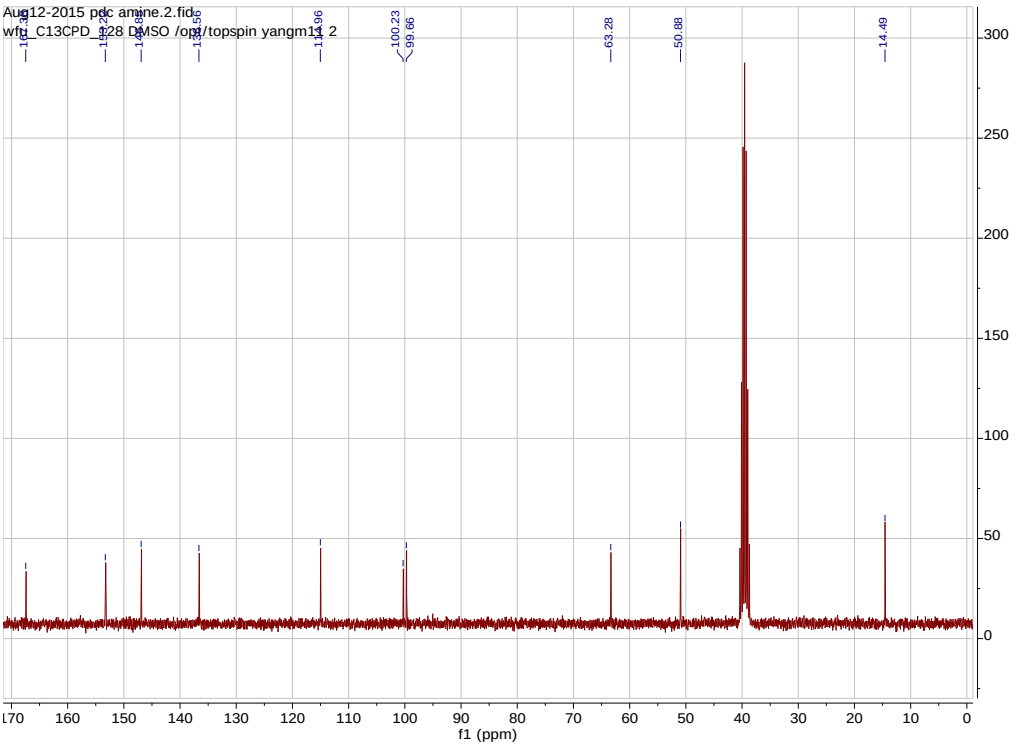

Figure S25. ^{13}C NMR spectrum of compound **1f** in DMSO-d_6.

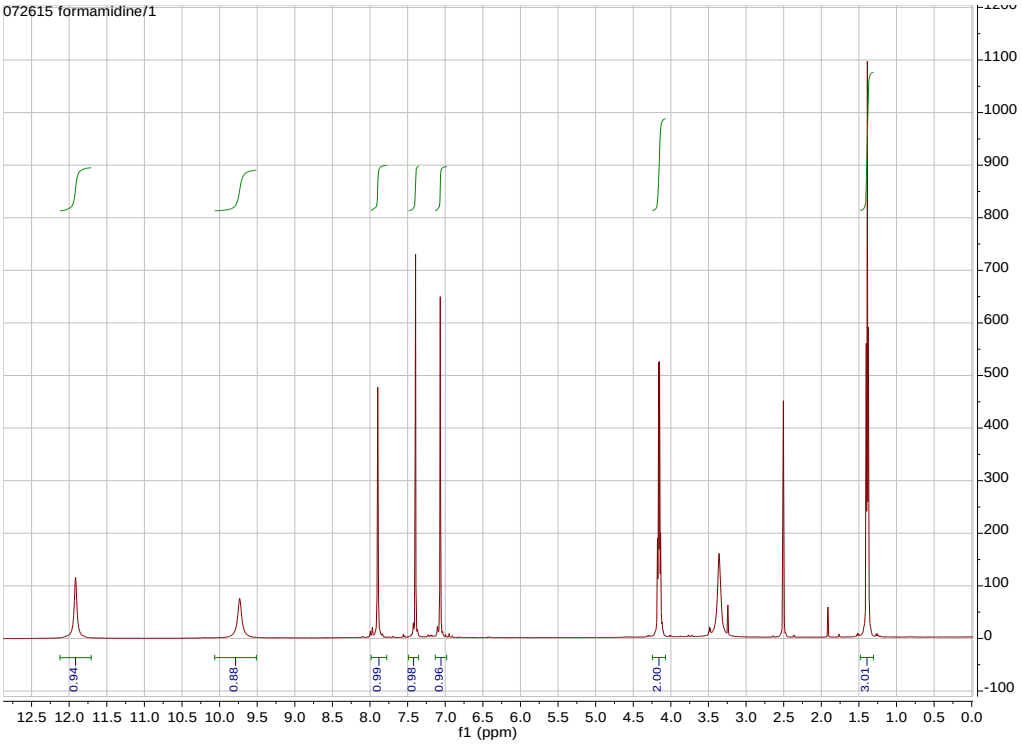

Figure S26. ^{1}H NMR spectrum of compound **1g** in DMSO-d_6.

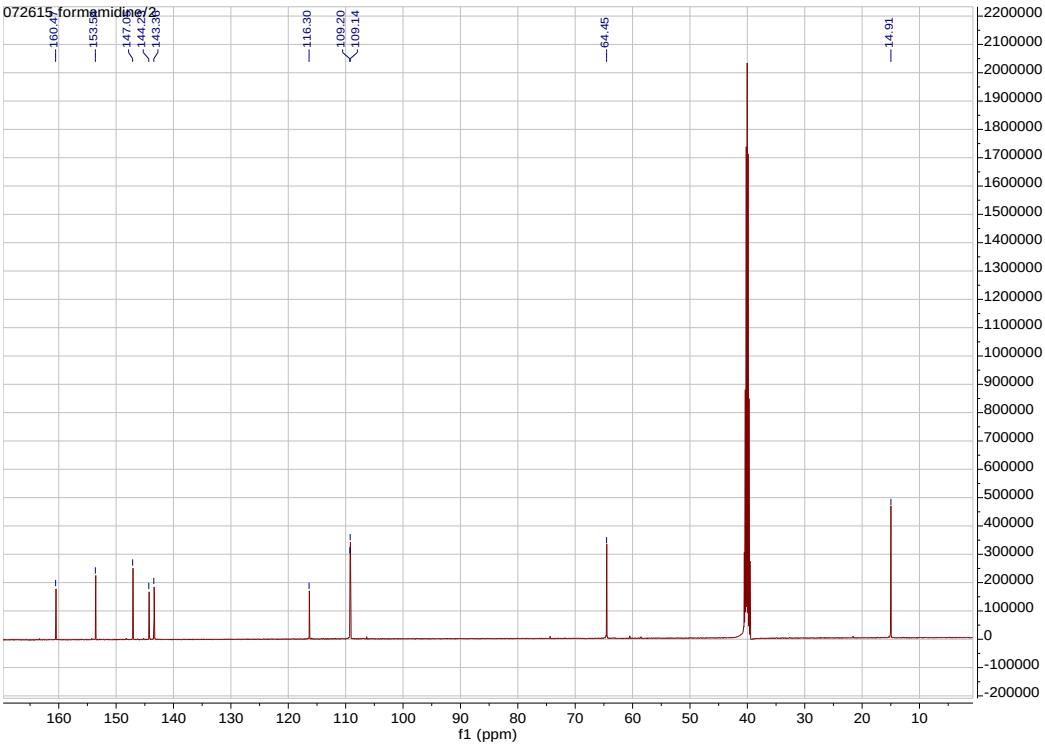

Figure S27. ^{13}C NMR spectrum of compound **1g** in DMSO-d_6.

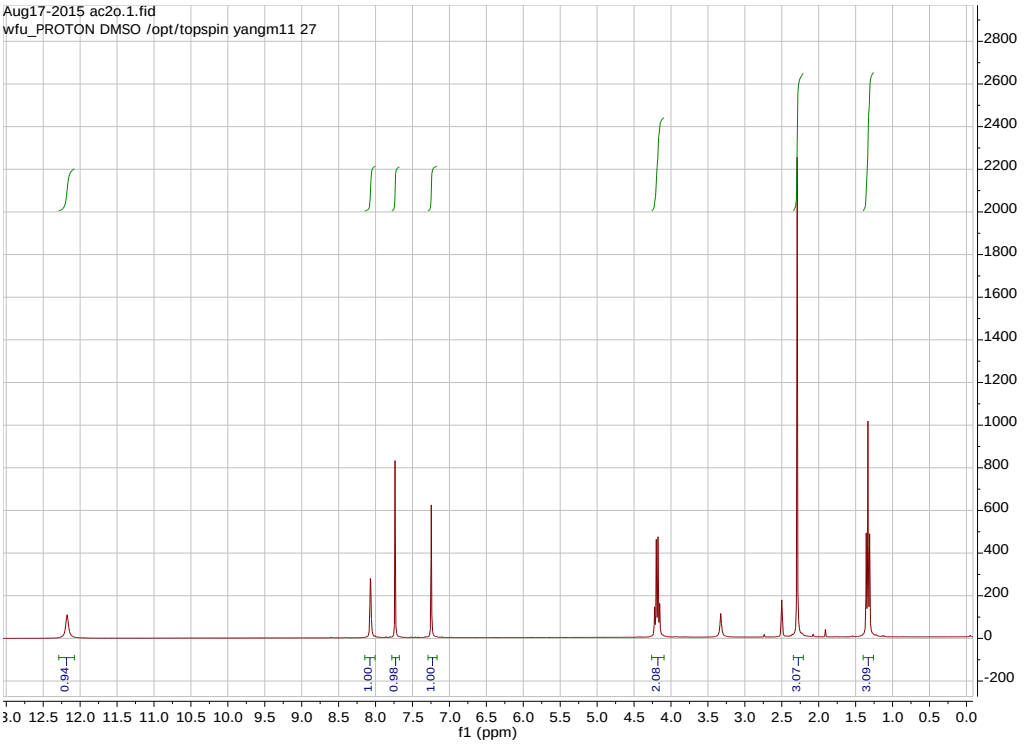

Figure S28. ^{1}H NMR spectrum of compound **1h** in DMSO-d_6.

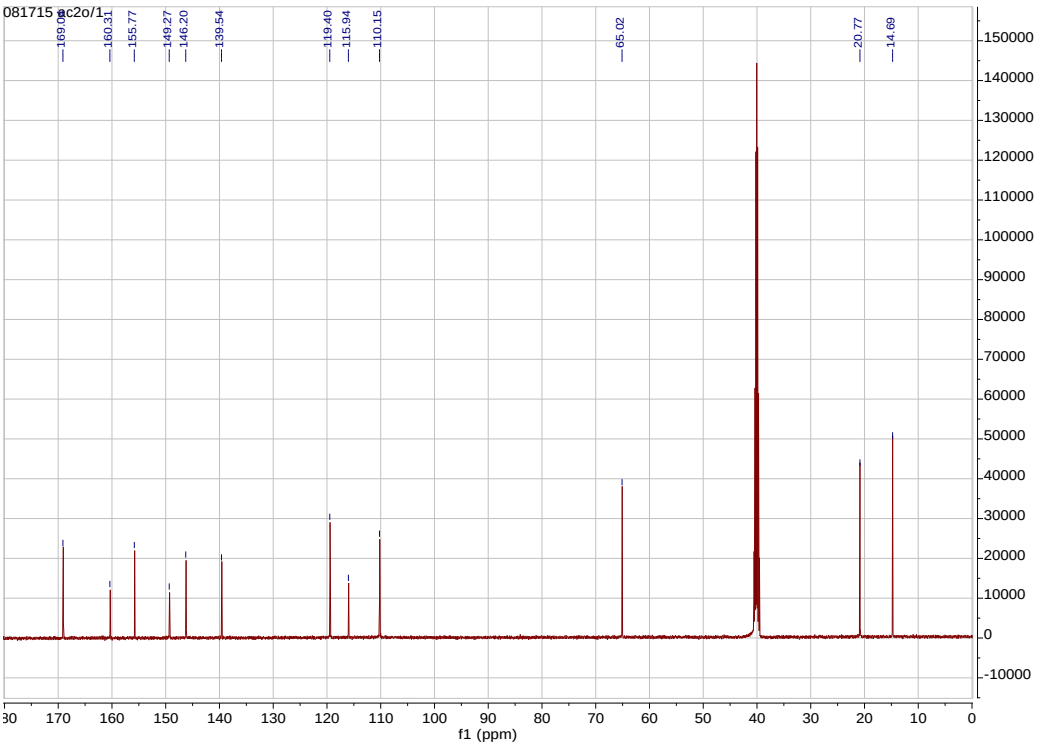

Figure S29. ^{13}C NMR spectrum of compound **1h** in DMSO-d_6.

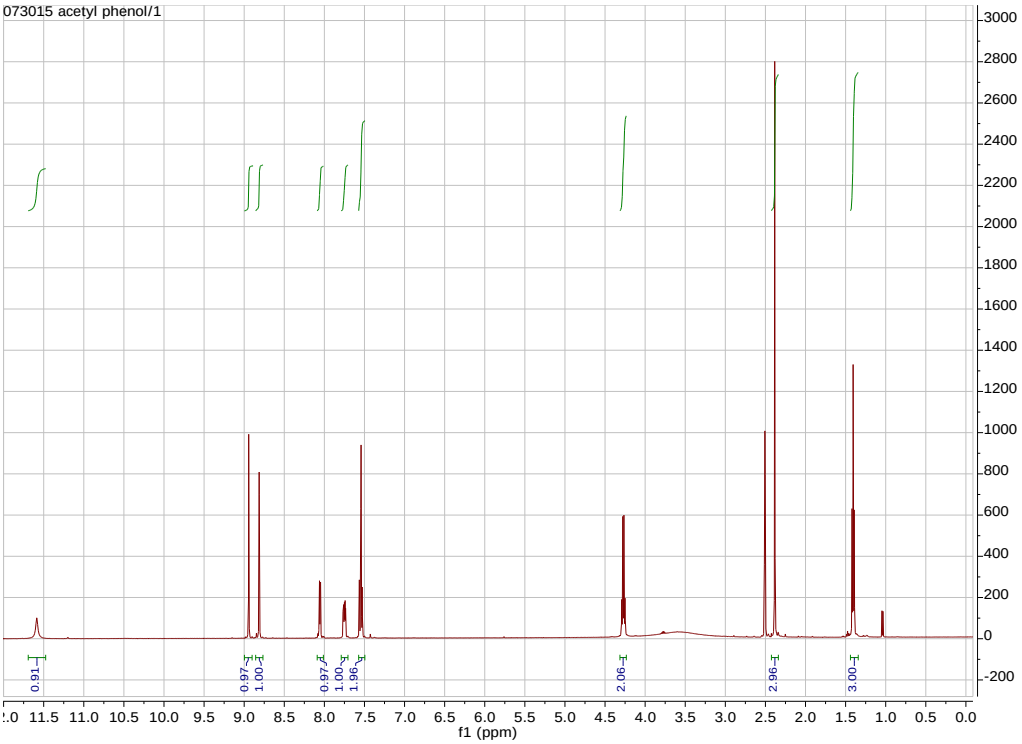

Figure S30. ^{1}H NMR spectrum of compound **1j**·HCl in DMSO-d_6.

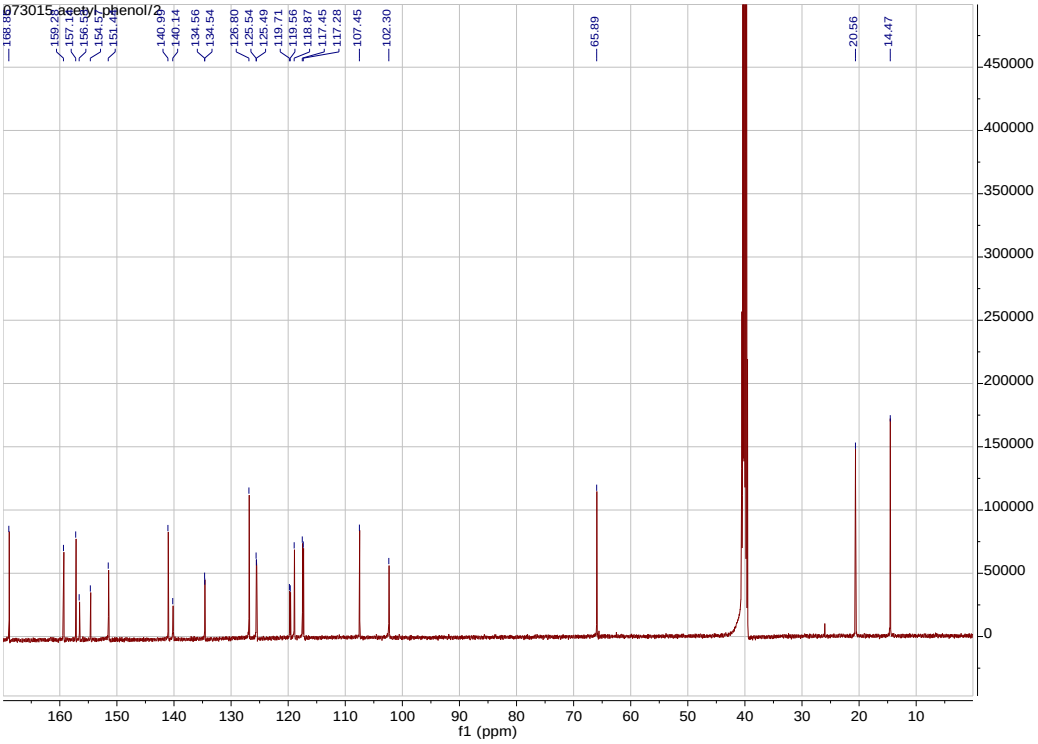

Figure S31. ^{13}C NMR spectrum of compound **1j**·HCl in DMSO-d_6.

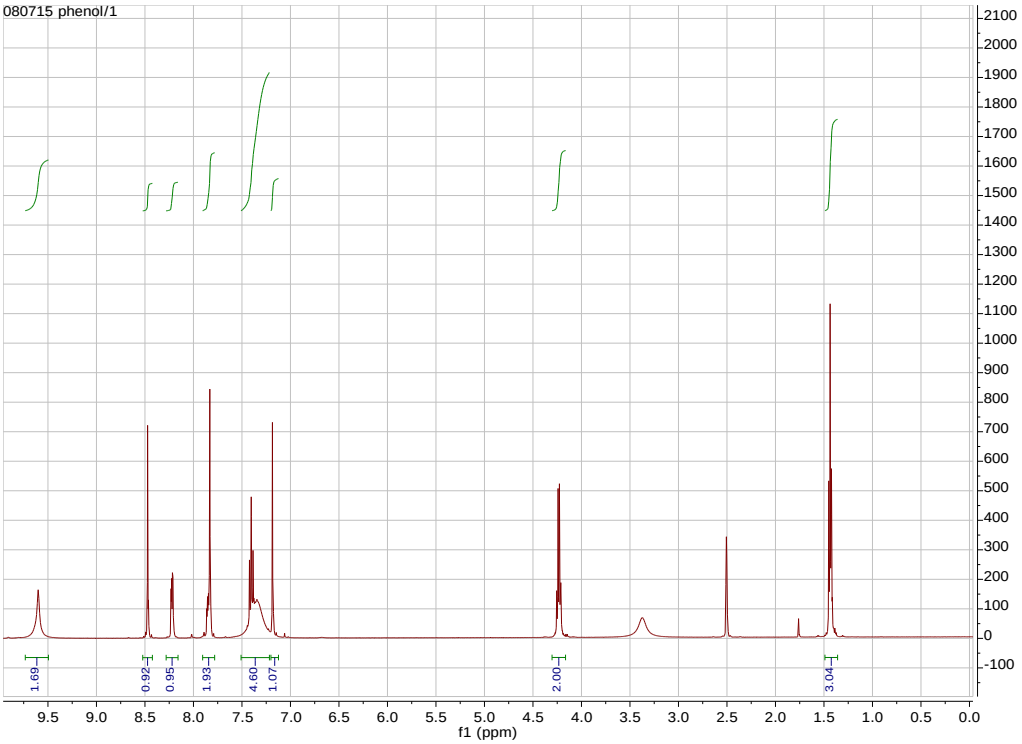

Figure S32. ^{1}H NMR spectrum of compound **1k** in DMSO-d_6.

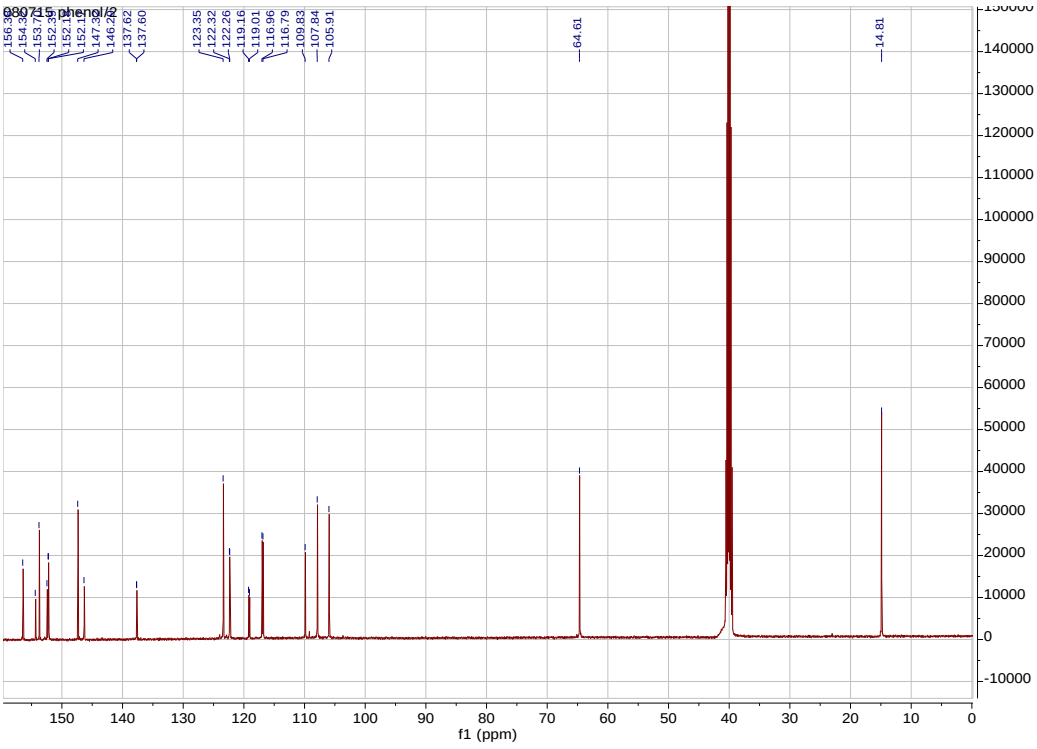

Figure S33. ^{13}C NMR spectrum of compound **1k** in DMSO-d_6.

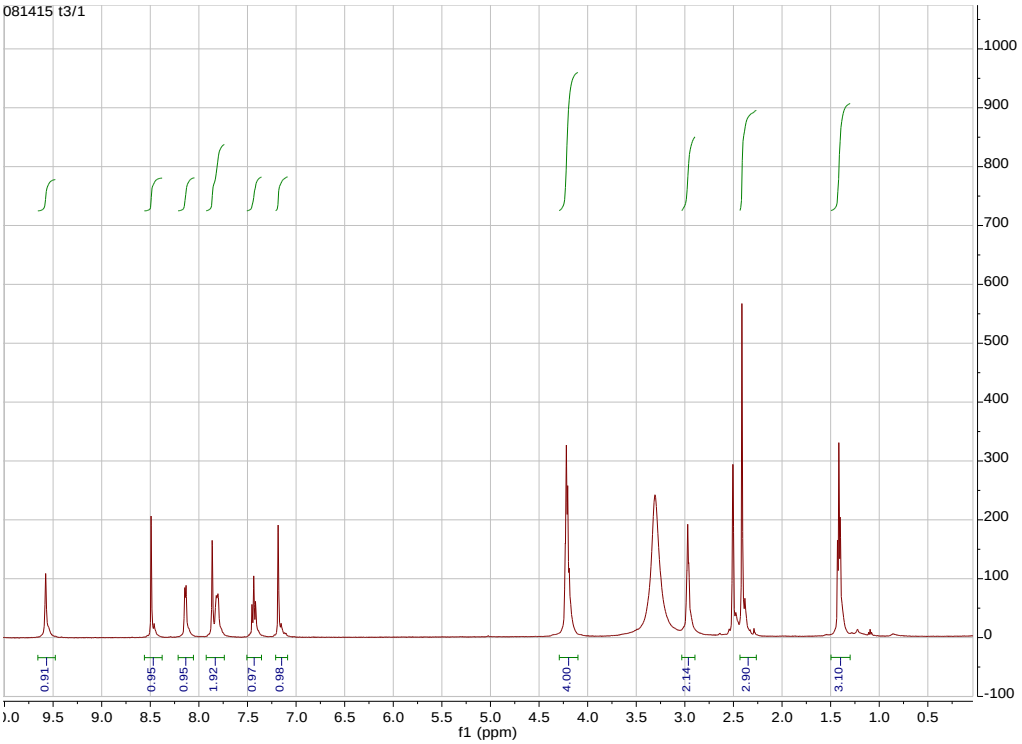

Figure S34. ^{1}H NMR spectrum of compound **1n (T2)** in DMSO-d_6.

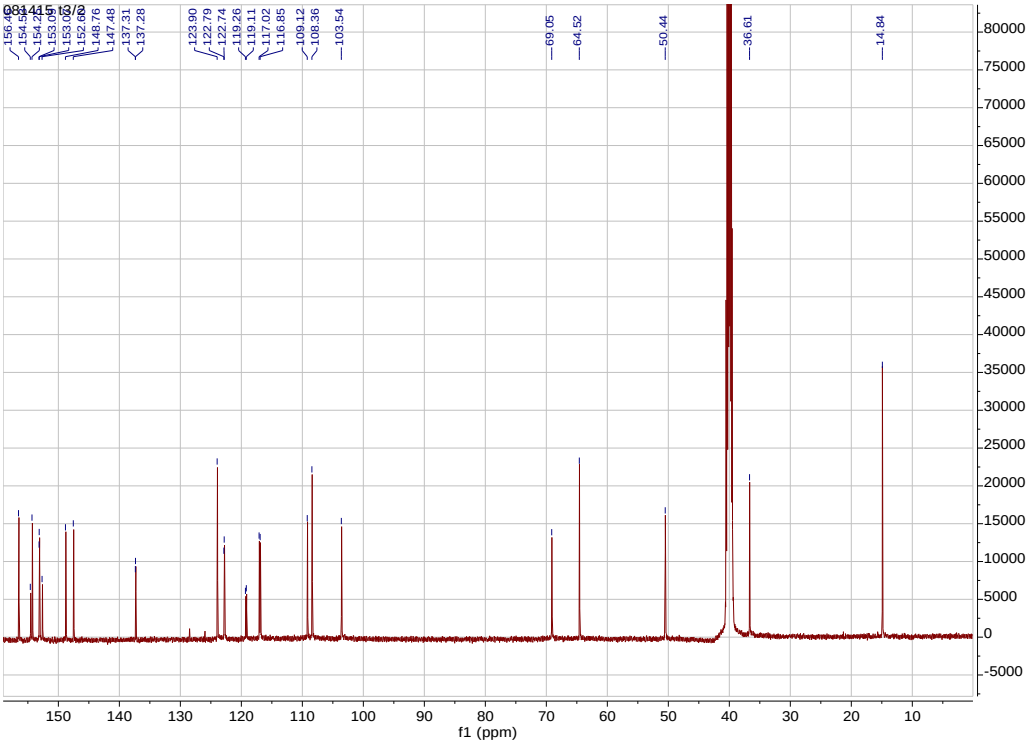

Figure S35. ^{13}C NMR spectrum of compound **1n (T2)** in DMSO-d_6.

6. References

1. A. P. Krapcho, E. Menta, A. Oliva, R. Di Domenico, L. Fiocchi, M. E. Maresch, C. E. Gallagher, M. P. Hacker, G. Beggiolin, F. C. Giuliani, G. Pezzoni and S. Spinelli, *J. Med. Chem.*, 1998, **41**, 5429-5444.
2. Q. Zhang, S. Dall'Angelo, I. N. Fleming, L. F. Schweiger, M. Zanda and D. O'Hagan, *Chem. Eur. J.*, 2016, **22**, 10998-11004.
3. A. Pickard, F. Liu, T. Bartenstein, L. Haines, K. Levine, G. Kucera and U. Bierbach, *Chem. Eur. J.*, 2014, **20**, 16174-16187.
4. M. Yang, A. J. Pickard, X. Qiao, M. J. Gueble, C. S. Day, G. L. Kucera and U. Bierbach, *Inorg. Chem.*, 2015, **54**, 3316-3324.
5. M. A. Fabian, W. H. Biggs, 3rd, D. K. Treiber, C. E. Atteridge, M. D. Azimioara, M. G. Benedetti, T. A. Carter, P. Ciceri, P. T. Edeen, M. Floyd, J. M. Ford, M. Galvin, J. L. Gerlach, R. M. Grotzfeld, S. Herrgard, D. E. Insko, M. A. Insko, A. G. Lai, J. M. Lelias, S. A. Mehta, Z. V. Milanov, A. M. Velasco, L. M. Wodicka, H. K. Patel, P. P. Zarrinkar and D. J. Lockhart, *Nat. Biotechnol.*, 2005, **23**, 329-336.